6-18-2019

Matrix Recharge in a Shrink-Swell Floodplain Forest Soil

Savannah R. Morales
smora22@outlook.com

MATRIX RECHARGE IN A SHRINK-SWELL FLOODPLAIN FOREST SOIL

A Thesis

Submitted to the Graduate Faculty of the
Louisiana State University and
Agricultural and Mechanical College
in partial fulfillment of the
requirements for the degree of
Masters of Science

in

The School of Renewable Natural Resources

by

Savannah R. Morales
B.S., Louisiana State University, 2017
August 2019

ACKNOWLEDGEMENTS

I would like to thank my committee members Drs. R. Keim, S. King, T. Quirk, and R. Stewart for your continued advice and feedback. A special thanks to my major advisor Dr. Keim for the freedom to tailor my research to fit my interests and non-traditional schedule, for the opportunity to improve my writing skills by writing and designing three separate experiment proposals (that was great), and of course, for the unique additions to my playlist. Thanks to lab mates and friends of the Keim Forest Ecohydrology Lab for the support and assistance: N. Nguyen, A. McAlhaney, A. Freeman, S. Bueche, S. Mootheart, M. Shockey, Stephen, Colby, and Dalton with a special thanks to M. G. Lemon for her assistance and continued guidance. Thank you, Jay Curole, for always making things happen. Thank you to the RNR Freshwater Ecology lab for your continued support and encouragement during my undergraduate and graduate days. A very special thank you goes out to Kayla Kimmel for being the friend and mentor I did not know I needed.

To my parents Charles and Patricia Morales: thank you for dip nets, fishing trips, microscopes, and pet nutria, owls, and raccoons. Thank you for your constant encouragement and for acknowledging that I am undoubtedly your favorite child. To the rest of my close family: thanks for always believing in me and being there when I needed you, I love you all and could not imagine life without you. To Colby, thanks for helping me cross the finish line. Thank you, Maw Maw Anna and Maw Maw Dora, for being what every little girl needs to look up to: a strong no-nonsense, tell it like it is, not afraid to get her hands dirty independent woman.

Most importantly I would like to thank my sons Bryce and JJ. You boys keep me moving and motivated. Thank you both for your involuntary help on multiple experiments and projects. Thank you, JJ, for teaching me that no matter how busy life gets, there is always time to stop and smell the flowers.

TABLE OF CONTENTS

ABSTRACT

Despite the global distribution of fine-grained Vertisols, the hydrology of these floodplain soils is still not well understood. Vertisols shrink and swell depending on soil moisture leading to a range of soil pore sizes, from large macropore cracks to smaller micropores, and consequently a range of hydraulic conductivities. Despite the plethora of research indicating the importance of both flooding and soil moisture in floodplain ecosystems, the specific role that flooding plays in soil moisture recharge has been less widely studied and remains of interest. Blue food dye and deuterated water were used as tracers to determine the role of the macropore network in matrix recharge under two artificial flood durations (3 days and 31 days) in large soil monoliths extracted from a fine-grained shrink-swell forested soil. Gravimetric soil moisture content increased by 41% in the first three days of artificial flooding and remained relatively constant with only a 3% increased from three to thirty-one days after flooding. Moisture content was greatest in the top 10 cm and relatively uniform from 10 to 75 cm depths. The proportion of artificial flood water continued to increase within the soil matrix throughout the course of the experiment. The proportion of matrix flood water was greatest at the surface and decreased with depth. Soil peds with greater connectivity to the soil crack network had greater proportions of artificial flood moisture. The results of this experiment indicate initial flooding dominates recharge and suggest flood frequency may be a more important factor in moisture recharge than flood duration in vertic floodplain soil.

INTRODUCTION

Fine-grained, floodplain Vertisols are globally distributed and occupy approximately 2.4% of the earth's non-ice-covered surface (USDA-NRCS, 1999). Fine-grained floodplains are utilized throughout the world for crop production and livestock grazing (Freebairn, 1986; Lal, 1987; Behera, 2007). These fine-grained vertic (shrinking and swelling) soils also support natural ecosystems such as grasslands and savannas in Africa (Fynn and Murray-Hudson, 2015), channel mudflats and annual monsoonal grassy floodplains in Australia (Gibling et al., 1998; Wurm, 2007), as well as bottomland hardwood forest (BLH) in Eastern Texas (Miller and Bragg, 2007) and the Lower Mississippi River Alluvial Valley (LMAV) (Aslan and Autin, 1999; King and Keeland, 1999; Hunter et al., 2008).

Despite global occurrence, the hydrology of these soils is not fully understood (Marshall et al, 1996; USDA-NRCS, 1999; Brady and Weil, 1999). The shrink-swell nature of Vertisols results in multiple flow paths that are dynamic in both space and time (Stewart et al., 2016), making hydrologic agricultural management decisions difficult and limits our understanding of eco-hydrological processes in undeveloped settings.

The shrink-swell dynamic is a function of soil moisture (Das Gupta et al., 2006; Romkens and Prasad, 2006; Stewart et al., 2016). At low moisture content the soil matrix shrinks, resulting in a heterogenous networks of cracks or macropores, in which flow is dominated by gravitational forces. At high moisture content the soil matrix swells, closing the macropore network. In Vertisols, macropores form the boundaries of soil peds, which are structured aggregates within the soil consisting largely of micropores, where water flow is dominated by capillary forces that hold water in tension (Marshall et al., 1996). Water flow processes in Vertisols are greatly influenced by pore size, which, can vary as a function of soil water content (Marshall et al., 1996; Brady and Weil, 1999).

Water movement in swelling and shrinking clay soils has been widely studied and models have been developed to quantify the flow rates for both matrix and macropore flow (Allen and Braud, 1966; Flury et al., 1994; Johnson et al., 1994; Romkens and Prasad, 2006; Hardie et al., 2013; Stewart et al., 2016). Many of these models were produced using data gathered from agricultural soils. While this research is important for understanding soil physics and dynamics, the resulting models are not necessarily representative of natural landscapes potentially containing a wider variety of soil conditions. *In situ* studies of water flux in forest soils are needed to add to the current body of knowledge regarding hydrology of fine-grained, shrink-swell soils.

Many crops and ecosystems are supported through dry seasons by high water-holding capacities of fine-textured soils (Virmani et al., 1982; Brady and Weil, 1999). Soil water is essential for sustaining these ecosystems, but the mechanisms by which these soils are hydrologically recharged are complex and poorly understood (Marshall et al., 1996; USDA-NRCS, 1999). Infiltration and flow in these soils has been found to vary with moisture content, depth, and time (Messing and Jarvis, 1990). In many Vertisols permeability is often low (Marshall et al., 1996; USDA-NRCS, 1999). Because of this, Vertisols have been known to be episaturated in some cases, meaning saturated at shallower depths and unsaturated at deeper depths (Pettry and Switzer, 1996; Slabaugh, 2006; Miller and Bragg, 2007).

Texture is not the only property influencing water flow in soil. Organic matter increases plant available water both directly due to high water holding capacity and indirectly because of the influence organic matter has on the structure and soil pore space. Soil structure is highly influential to hydraulic conductivity because water passes quickly through large macropores and more slowly through micropores (Marshall et al., 1996; Brady and Weil, 1999). In shrink-swell soils, time and moisture content jointly influence conductivity as the matrix-macropore network changes (Marshall et al., 1996; Brady and Weil, 1999; Farve et al., 1997).

Time dependence of crack closure and soil expansion was demonstrated by Favre et al. (1997) when upon wetting a dry and cracked Vertisol, the soil matrix continued to swell even after the cracks had closed. These findings demonstrate how hydraulic conductivity (K_{sat}) shifts from predominantly mass flux water movement to micropore flow as the soil matrix swells and the crack network closes upon wet-up.

Flood duration plays a crucial role in influencing floodplain ecosystems. Flood duration has been found to influence vegetative productivity, species composition, and species distribution in BLH forests (Broadfoot and Williston, 1973; De Jager et al., 2012). Extended flooding can lead to anoxic soils, cause mortality, and prevent or limit tree regeneration (Kroschel et al., 2016; Krzywicka, et al., 2017). Despite the known significance, the role of flood duration and effects of ponding on soil moisture recharge, specifically in Vertisols, is less well understood.

Stable water isotopes deuterium and ^{18}O are commonly used as conservative tracers to distinguish water pools and sources (Kendall and McDonnell, 1998; Garvelmann et al., 2012). Brooks et al. (2010) and Goldsmith et al. (2012) found the isotopic signatures of bulk soil water and plant water did not match rainwater. In less than a decade multiple ecohydrological researchers have published similar findings from numerous systems (Evaristo et al., 2015; Berry et al., 2017; Geris et al., 2017). This phenomenon has been coined the “Two Water Worlds” hypothesis (TWW), and holds that water used by plants and terrestrial ecosystems may be part of a separate water cycle than runoff. Given the shrink-swell nature of clay Vertisols and their spectrum of hydraulic conductivities, BLH forest may be a system in which the translatory flow model is not an accurate depiction of the soil hydrology. It is just now becoming apparent the degree to which understanding links between water flowpaths and recharge of matrix water may be critical for ecosystem functioning. In BLH, these linkages may be crucial in supporting tree growth during droughts (King and Keim, 2019).

Dyes have been used to map and distinguish various soil flow paths (Flury et al., 1994; Ketelsen and Meyer-Windel, 1999; Weiler and Flühler, 2004; Hardie et al., 2013). Flury et al. (1994) used blue food dye to assess the flow paths on 14 field sites and concluded most water bypassed the soil matrix through preferential macropore flow paths. Ritchie et al. (1972) used fluorescein on a swelling Houston black clay and found preferential flow paths were active even under saturated conditions, flow was not evenly distributed, and much of the matrix water was not active in flow when compared to flow around structured aggregates.

The uniqueness of the expansive (vertic) soils has long been recognized in fields including engineering, agriculture, and forestry (Broadfoot, 1962; Hillel, 1998; Jones and Jefferson, 2012). Here I attempt to distinguish the influence of macropore connectivity on matrix recharge in a vertic floodplain forest soil under two different flood durations. Data gathered from this experiment may influence soil hydration model parameters, floodplain management decisions, and address the TWW hypothesis and possibility in this system.

RESEARCH OBJECTIVES

Broad Objective: The larger scope of this experiment is to extend the current knowledge of floodplain hydrology in vertic, clay soils.

Research Question: How does the macropore network function to recharge the matrix in forested shrink-swell soils?

Specific Objectives: I will (1) use Brilliant Blue FCF dye tracing to estimate connectedness of individual peds to the macropore network at multiple depths in the soil profile and (2) use stable water isotopes to determine whether water is incorporated at different rates for various depths throughout the soil profile and determine whether ped organic content and/or macropore connectivity is correlated with post treatment water content.

METHODS

To conduct this experiment, 6 soil monoliths were excavated from a shrink-swell clay forest soil (4 treatment monoliths and 2 control monoliths). The treatment monoliths were submerged in dyed and isotopically spiked tap water for a short and long artificial flood duration. After treatment, the monoliths were deconstructed to extract individual peds that were then measured for dye coverage, stable water isotopes, moisture content, and organic matter. Control monoliths were deconstructed into peds and initial moisture content, organic matter, and initial isotopic composition were obtained. Data collected from control peds were used as a surrogate for pre-treatment field conditions in the treatment monoliths, which could not be measured without disturbing the monoliths.

STUDY SITE

The study site is a BLH in the LMAV near St. Gabriel, Louisiana approximately 10 km south of Baton Rouge (30°16'54"N, 91°05'21"W). This forest, as well as the surrounding landscape, was disconnected from flooding by the Mississippi River by 1812 due to levee construction. Although the site no longer receives overbank flooding from the Mississippi River it continues to receive backwater flooding from rivers to the east and north of the site, and by ponding of local rainfall. It is frequently inundated during the late winter through spring (January-May) and relatively dry during the summer months (May-October). The annual precipitation for the area is approximately 158 cm. The site has been logged on multiple occasions, but has remained relatively undisturbed, except for partial cuts, since around 1950. The soil is mapped by NRCS (2017) as Sharkey, clay, 0-1 percent slopes, frequently flooded, very-fine, smectitic, thermic Chromic Epiaquerts (NCSS, 2013).

FIELD SAMPLING

Four soil monoliths approximately 50 cm^3 were excavated from depths of 0-35 cm and 40-75 cm. Care was taken to ensure the soil remained as intact and undisturbed as possible. This was done by gently excavating the soil surrounding the monolith until the desired size was achieved (Figs. 1, A.1, and A.2). The monoliths were then transferred to metal containers (each was one half of a 125 L (33-gallon) steel drum open on the top and pre-drilled with one cm diameter holes spaced five to eight centimeters apart on the bottom and sides to allow relatively free ingress of water) and wrapped in plastic to prevent soil water evaporation during transportation to the lab. Two smaller 19 L (5-gallon bucket sized) monoliths were excavated from 0-35 cm and 40-75 cm depths and plastic wrapped to provide control samples.

Figure 1. Excavation of soil monolith. Soil was excavated around monolith to fit inside half of a 33-gallon steel drum.

LABORATORY METHODS

To determine macropore-matrix connectivity and water exchange during flooding, two tracers were added to two 208 L (55-gallon) steel drums that served as flood treatment tanks for the 4 soil monoliths. FD&C Blue #1 (C.I. 42090; Brilliant Blue FCF; C.I. Food Blue 2) was used in concentrations of 1 g L^{-1} as a semi-quantitative visual tracer for macropore connectivity. This concentration is lower than many soil dye experiments (Flury et al., 1994; Flury and Fluhler, 1995; Weiler and Fluhler, 2004; and Hardie et al., 2013) due to the lack of depth the dye needed to reach and the amount of time the soil was to be submerged in the solution. Blue FD&C dye is commonly used as a hydrologic tracer for visualizing flow paths because it sorbs to soil surfaces (Flury and Flühler, 1995; Ketelsen and Mayer-Windel, 1999; Öhrström et al., 2004). Non-sorbing, conservative tracers, deuterium and ^{18}O in water, were used to trace water movement and source water proportions in flood peds. Deuterated water (98 at. %) was used to spike the tap water to values well above natural field conditions: drum A (short duration flooding) had, $\delta D = +68 \pm 1‰$ and drum B (long duration flooding) had, $\delta D = +70 \pm 1‰$ Vienna Standard Mean Ocean Water. The ^{18}O content of the flood water was tap water; for both drums A and B $\delta O^{18} = -5 \pm 1‰$. All isotope values are reported using δ of D or ^{18}O of liquid water in per mil (‰) relative to Vienna Standard Mean Ocean Water (VSMOW) following the expression:

$$\delta^{18}O \text{ or } \delta D = \left(\frac{R_{sample}}{R_{standard}} - 1\right) * 1000, \quad (1)$$

where R= heavy/ light isotopic species of ^{18}O or deuterium.

On the same day as excavation, the four treatment monoliths in their smaller metal containers were unwrapped from plastic and lowered into the barrels, with the containers holding the 40-75 cm depth monoliths placed on the bottom and the shallower monoliths resting on top of the containers holding the lower monoliths with a wooden spacer of approximately 5 cm (Figs. 2 and 3). All soil was fully submerged, simulating a flood of 2-4 cm depth above the soil surface. The drums were then sealed to prevent evaporation.

Figure 2. Soil monolith being lowered into treatment water with the aid of an engine hoist.

Drum A soil monoliths, i.e., the short treatment, remained submerged for 3 (shallow monolith, 0-35 cm) and 4 (deep monolith, 40-75 cm) days. On the third day of submersion the shallower soil monolith was removed and processed to measure dye coverage, wet weight, and water isotopes of individual peds. The 40-75 cm monolith was processed the same way the following day. It was not feasible to process both monoliths on the same day due to time constraints. Drum B soil monoliths, i.e., the long treatment, remained submerged for 31 and 32 days. Processing methods were the same for both treatment durations

Once the monoliths had reached the designated flood durations they were removed from the treatment barrels using an engine hoist and allowed to freely drain for approximately 20 minutes. The monoliths were then taken to the lab for ped separation. Each monolith was manually deconstructed by separating peds along natural lines of fracture to obtain treatment peds for analysis of dye coverage and δD (Figures A3-A9). During ped excavation care was taken to reduce evaporative fractionation of soil water. Exterior soil, 2-3 cm on top, bottom, and sides, was considered disturbed and was discarded. The thin (<1 cm) O horizon was discarded as well. Peds were obtained from depth classes 0-4, 4-10, 10-20, 20-35, 40-55, and 50-75 cm to reflect variability in the soil profile. The soil properties in the upper 20 cm varied in structure more than below 20 cm, and smaller depth classes were designated there to account for this variability. Ped excavation was performed using a knife tip and gently plucking out naturally structured peds. Peds that broke or seemed disturbed were discarded. Care was taken not to smear the soil or otherwise alter the ped surface. In total, 339 flooded peds were obtained.

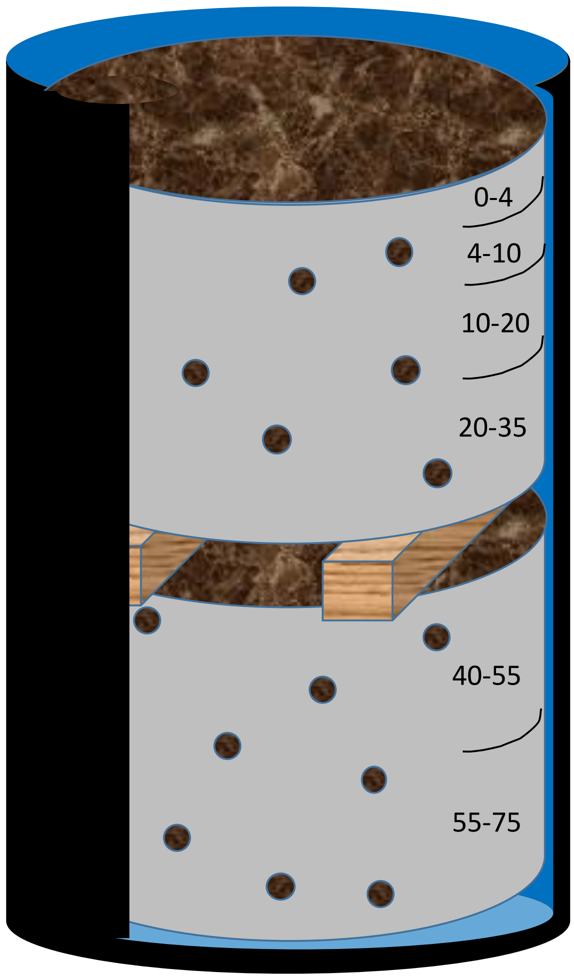

Figure 3. Schematic of treatment barrel set-up. Numbers depict depth classes in cm. Set-up was identical for both short and long treatment barrels.

Once a flood ped was obtained, it was visually inspected and assigned a dye coverage class of 0-20, 21-40, 41-60, 61-80, or 81-100 percent dye coverage. Throughout ped excavation dye coverage was inspected and assigned by the same person to insure constancy.

After dye coverage estimation, each ped was immediately placed into a pre-weighed, 10 L, side-gusseted coffee bag (PBFY Flexible Packaging; Gralher et al., 2018) and partially heat sealed for isotopic equilibration between soil water and vapor, using a method adapted from Wassenaar et al. (2008). The bag containing the ped was then weighed, inflated with ambient air, fully heat sealed, and inspected for leaks. The inflated ped bags equilibrated for 2-3 days in the same room as the laser water vapor isotope analyzer (LWIA) that was used to analyze vapor in the bags (LGR IWA-45-EP). Bags containing standards for calibration were made on the same day and following the same method as the ped bags. Recording thermometers (ONSET HOBO data loggers) recorded the room temperature every 15 or 30 minutes during this equilibration period to (1) ensure consistency of temperature and thus equilibration between water and vapor, and (2) allow estimation of α, the temperature-dependent equilibration factor between vapor and liquid in a closed system. Precision of the LWIA in this experiment is ±1 ‰, estimated as the variance in values obtained by analyzing bags containing standards analyzed as samples.

To infer δD soil water from δD vapor measurements, we used the free-liquid alpha (α) (Majoube, 1971) and empirical calibration obtained by adding water of known isotopic composition to otherwise-empty bags and measuring vapor the same way as for soil peds. We did not correct for fractionation known to occur by sorbing water onto surfaces (Lin and Horita, 2016; Lin et al., 2018; Oerter et al., 2014) or by hydration of solutes (Oerter et al., 2014). Ignoring these effects likely caused up to approximately 6 to 8 ‰ error, but this possible error is much smaller than the difference between pre-experiment water and the spiked floodwater.

It is possible that isotopic equilibration between water in peds and in the vapor of the bag preferentially involved water near the surface of peds. If that were the case, the isitopes of the vapor would potentially not reflect the isotopes of the liquid in the entire ped. To assess this possibility a separate experiment was conducted to test (1) whether the peds were fully equilibrating in the vapor bag during isotopic analysis and (2) whether any disequilibrium was related to ped size. Sample soil was collected from the study site and separated into a control and a treatment batch. The control soil was separated into peds and processed using the same vapor bag equilibration method as the main control soils with the exception that, of the 31 control peds, 16 were crumbled before being placed inside of the vapor bag and 15 were left whole and placed inside the vapor bags, as were the sampled peds for the main experiment. The treatment batch soil was dunked into isotopically spiked ($\delta D = +68$ ‰) and dyed tap water and allowed to soak for 24 hours. The treatment soil was then gently broken apart yielding 44 treatment peds. Of the 44 treatment peds, 22 were crumbled before being placed in vapor bags, and 22 were left whole, as were the control peds and the treatment peds for the main experiment. A Welch two sample t-test was used to test the null hypothesis of no difference in isotopic composition of vapor inside the bags between the whole and crumbled groups of the controls and treatments. The control group had no significant difference between the crumbled and whole peds, which would be expected, ($p=0.8$, crumbled $\bar{x} = -16 \pm 1$ ‰, whole $\bar{x} = -16 \pm 1$ ‰).There was high variance in the treatment group, but no significant difference between the crumbled and whole peds ($p=0.3$, crumbled $\bar{x} = +6 \pm 20$ ‰, whole $\bar{x} = 0 \pm 18$ ‰). The high range of values in the treatment batch may have reflected the positions of the ped within the soil monolith during soaking. Given these results, we concluded that sampling whole, non-crumbled peds did not bias the isotopic results. All statistical analysis was performed using RStudio version 1.1.456.

PHYSICAL PROPERTIES OF SAMPLED PEDS

After measuring dye coverage and stable water isotopes, each ped was processed to obtain soil physical properties, included fresh weight (field weight for controls and post-treatment ped weight for treatment peds), oven dry weight, percent organic matter (percent mass loss on ignition), and particle size distribution. Methods described by Klute (1986) were used to determine oven dry weight, water content, and percent organic matter. Oven dry weight was found by drying the soil peds at 105° C for a minimum of 24 hours until there was less than 3 percent change in weight between consecutive measurements. All soil water contents were recorded gravimetrically as is customarily done with Vertisols. Organic matter content was determined for each ped using the loss on ignition (LOI) method (Howard, 1965). Oven-dried peds were re-weighed, combusted at 550° C for two hours, allowed to cool within the furnace, and then weighed again. Particle size analysis (PSA) was performed for each depth class using a laser diffraction particle size analyzer (Microtrac S3500) (Jena et al., 2013). For PSA analysis 20 g of sample soil from each depth class was added to 150 mL of DI water in an electric mixer and mixed for five minutes. The soil-water mix was then poured over a 2 mm sieve to remove large organic matter and oven dried overnight to remove excess water. Small organic matter was then removed by mixing dried soil sample with 30% H_2O_2 and DI water repeatedly, in 5-7 minute intervals, until excessive frothing ceased (Klute, 1986). After organic matter was removed the soil was oven dried. Approximately 0.5 g of dried soil was added to 18 mL of DI water mixed with 4 mL of sodium hexametaphosphate and shaken to deflocculated any aggregates. The Microtrac was set to estimate particle size assuming irregular shape, transparent absorption coefficient (Özer et al., 2010), and a preset refractive index for clay.

It was not possible to obtain pre-treatment physical properties of flooded soil peds without disturbing the treatment monoliths, so control peds were used to gather pre-treatment, field conditions of the soil. Control soil was stored in the lab overnight after soil excavation from the field, covered in plastic wrap to prevent evaporation, and processed the next day. Control peds were processed using the same methods as flood peds except depth classes were 0-4 cm, 4-35 cm, and 45-55 cm. In total, 53 control peds were obtained.

Control peds were used to estimate pre-flood gravimetric water content and δD. To account for natural variability three different scenarios were used and estimated; moisture content equal to the mean, minimum, or maximum initial moisture content and δD of soil water for flood peds using polynomial regression (Fig. 4A). The δD expected by mass flux of flood water was calculated by assuming all additional moisture was from flood water, and assuming initial moisture was either the minimum, mean, or maximum of control peds. Moisture addition after dunking was calculated by the difference between initial estimated moisture content and post-flood moisture content (wet ped weight). Measured δD in flooded peds was compared against expected δD.

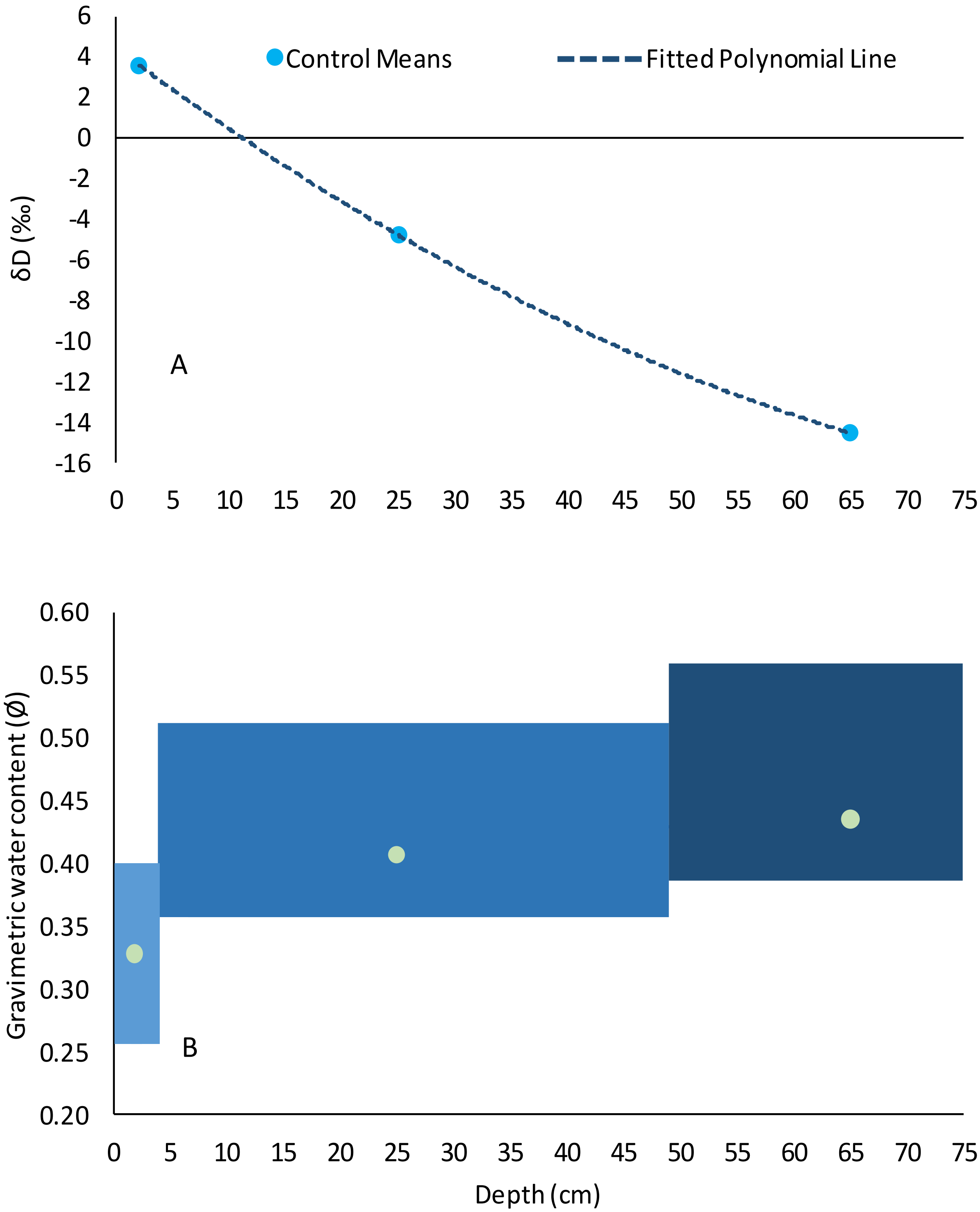

Figure 4. (A) Mean depth and δD of control peds plotted with polynomial line used to estimate pre-treatment control δD for each depth class. (B) Mean and ranges of control gravimetric moisture content. Plotted points represent mean moisture contents for depth classes 0-4 cm, 4-45 cm, and 45-75cm; boxes represent the range moisture across each control depth class.

RESULTS

During excavation the soil was relatively dry and visibly cracked on the surface. Many fine to medium sized roots were present, especially in the top 40 cm, but no large roots were present in any of the monoliths. Free flowing water was not observed. Soil texture was approximately 2% sand, 60% silt, and 38% clay (Table B.1), using the USDA texture size classes of clay ≤ 2.00 µm. The silt was very fine and most bordered on clay size: 15 percent of the particles were between 2 and 3 µm. The soil was composed of wedge-shaped peds bounded by failure planes and slickensides, consistent with formation by shear failure during repeated shrink-swell action (Brady and Weil, 1999).

A total of 392 usable peds were collected, including 53 controls, 162 short flood duration peds, and 177 long flood duration peds. At shallower depths, peds were smaller and broke apart more readily than deeper peds, which made it harder to collect distinct peds near the surface. Small, "buckshot" (Broadfoot, 1962) aggregates were common near the surface. Sampled ped weight varied little by depth (Fig. 5), although this was influenced by methodological procedures requiring peds of at least 3 g to provide sufficient water for isotopic analysis. Deeper than 20 cm, the soil contained more slickensides and peds readily separated. Ped boundaries tended to be formed on sides of medium-sized roots, and there were no peds formed completely around medium roots. Fine roots (≤ 2 mm) were found within peds.

Artificial flooding caused gravimetric moisture content to increase from 0.40 ± 0.05 (mean ± SD) g/g in the control peds to 0.59 ±0.07 in the first 3 and 4 days (short flood, +41% change) and increase from 0.59 ±0.07 to only 0.62 ± 0.08 from 3 to 31 days (short to long flood; +3% change, Fig. 6). Although soil moisture increased between flood durations, the difference was much smaller than the effect of the initial flood. Gravimetric moisture content in the control soil increased with depth ($R^2 = 0.37$, $p < 0.001$, $\beta = 0.001$, linear regression). Moisture content in the flooded peds decreased with depth for both flood durations ($R^2 = 0.13$, $p < 0.001$, $\beta = -0.001$ short flood; $R^2 = 0.15$, $p < 0.001$, $\beta = -0.001$, long flood; linear regression). By depth class there was a significant increase in gravimetric moisture content from short to long flood durations for depth classes 4-10, 10-20, 20-35, and 55-75 cm only (all $p < 0.014$, student's t-test). There was no difference in gravimetric moisture between durations for depths 0-4 cm ($p = 0.166$, student's t-test) and 40-55 cm ($p = 0.084$, two sample t-test). Due to experimental design, the surfaces of depth classes 0-4 cm and 40-55 cm were both more exposed to treatment water and under less confining pressure from the surrounding soil than the other depth classes, and thus there was room for those peds to expand and increase moisture.

Figure 5. Fresh ped weights (g) by depth class for both short (3 and 4 days) and long (30 and 31

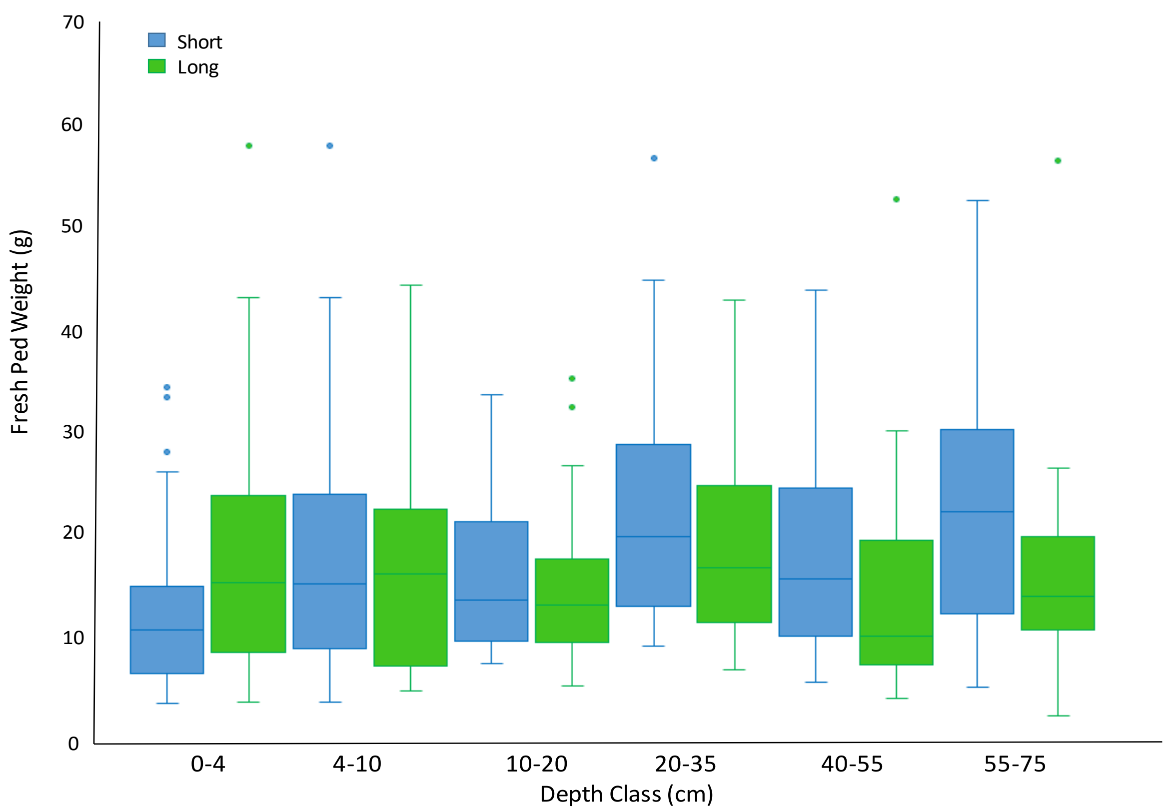

days) duration. Ped weights were uniform throughout the profile.

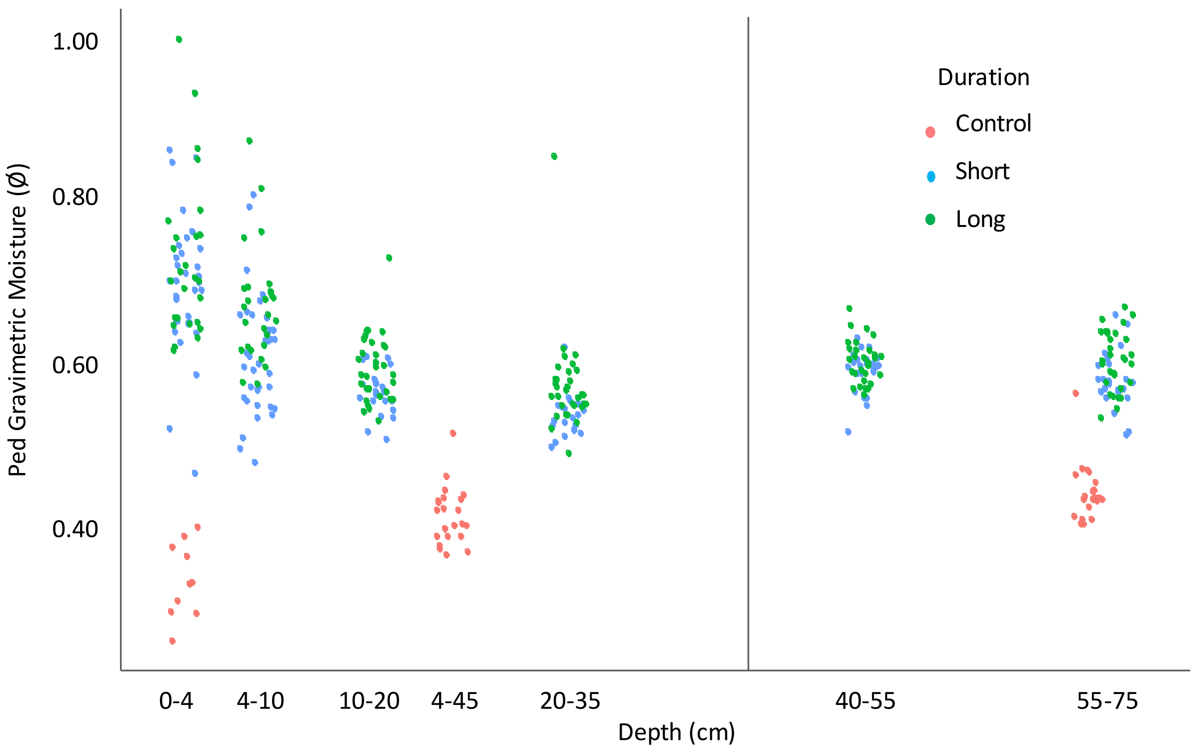

Figure 6. Gravimetric moisture content by depth for all peds.

Percent organic matter decreased with depth across all peds (R^2 = 0.48, p<0.001, β =-0.06, linear regression; Fig. 7). There was no difference in percent organic matter between short and long flood duration peds (p = 0.48, Welch t-test), which was expected. Control peds had less organic matter (control $\bar{x}$ = 6.46 ± 1%; combined flooded $\bar{x}$ = 7.40 ± 2 %, p < 0.001, Welch t-test) than flooded peds. Control and flooded soil were gathered in the same location; this statistical difference is likely due to random chance. Gravimetric moisture increased with increasing organic matter for both flood durations (R^2= 0.64, p<0.001, β = 0.03, and R^2 = 0.56, p<0.001, β = 0.04, short and long respectably, linear regression), but decreased with increasing organic matter in the control peds (R^2= 0.32, p<0.001; β = -0.02, linear regression; Fig. 8).

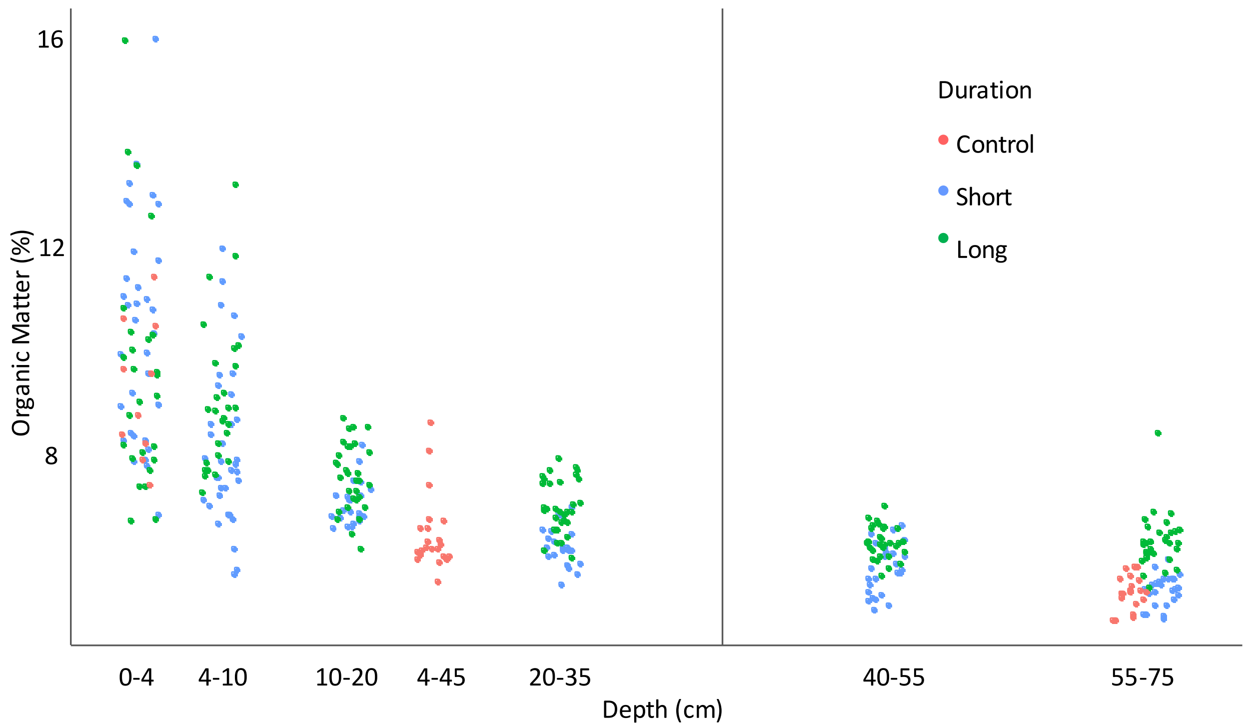

Figure 7. Percent organic matter by depth for all soil peds.

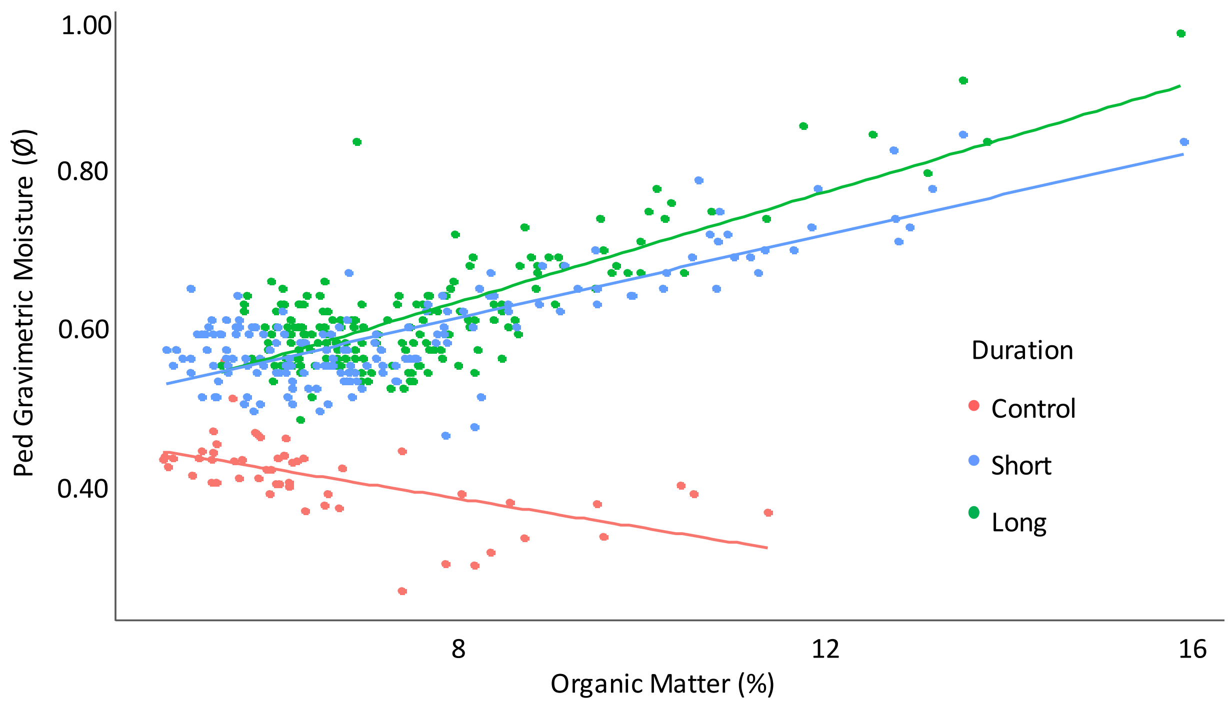

Figure 8. Scatterplot of ped percent organic matter (g organic matter/ pre-combustion total ped weight) Vs ped gravimetric moisture content (g water/ g oven dry soil). Linear regression lines for each duration are included. Flooded and field soil display opposite trends, this is due to lower water contents in surface control peds from evaporation.

In general, and for both flood durations, dye coverage on ped surfaces became less as depth increased. Dye penetration did not occur more than a few mm into the soil matrix (Fig. A.6). For both durations, dye coverage on surface peds was greatest in the 0-4 cm depth class and least in the 44-55 cm depth class (Fig. 9.A and 9.B). There was no distinct pattern in differences of dye coverage occurance with depth between flood durations (Fig. 9.C).

The ped water was heavier in δD (i.e., greater percentage of flood water in ped) for the long flood duration than the short duration across all depth classes. Depth class 0-4 cm had the smallest difference in δD between durations. For all depth classes, except 20-30 cm, the range of ped δD was greater for the short duration. The δD of depth class 40-55 cm (the top of the lower monolith) was highly variable in the short duration and less so in the long duration (Fig 10). The mean δD in the flooded peds was greater for the long duration than for the short ($p<0.001$, short $\bar{x}$= +41‰, long $\bar{x}$= +59‰, student's t-test).

Measured δD was consistently higher (i.e., apparently more flood water) than the calculated expected δD given moisture content increase (Fig. 11). Although δD decreased with increasing depth in the control peds, those variations were small relative to the effects of the tracer addition. based on soil moisture change by dunking for peds exposed to long-duration flooding. In the short flood duration, measured δD was more variable; some samples fell within the expected range and some exceeded the expected deuterium concentrations (Fig. 11). Deuterium content increased with dye coverage for both flood durations (Fig 12). The short artificial flood duration showed a greater range in δD than the long duration. The long artificial flood duration was more similar to treatment water (long flood water = +70 ‰).

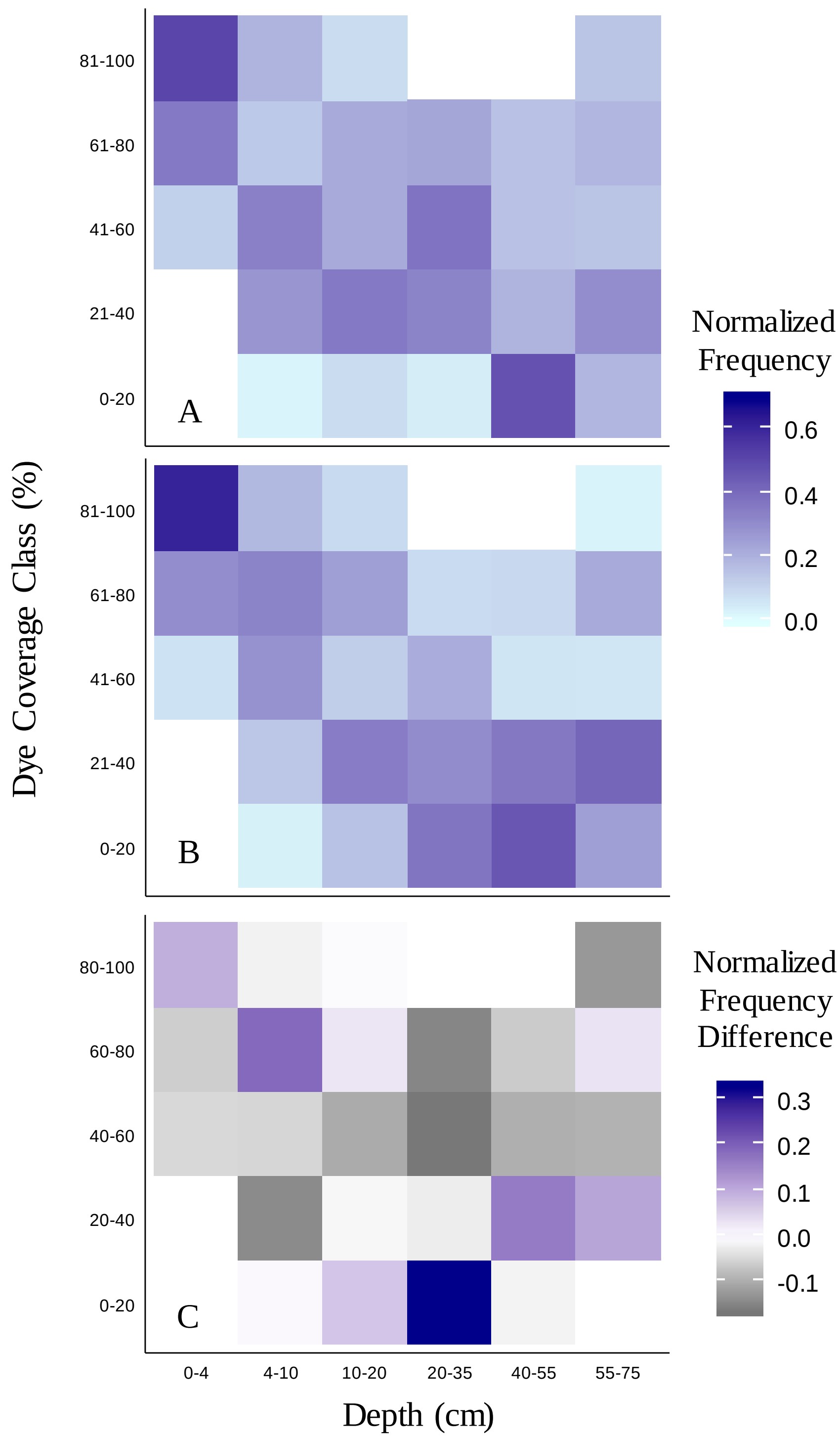

Figure 9. Histogram plots depicting normalized (by depth class) number of peds for each depth by dye coverage category for (A) short flood treatment, (B) long flood treatment and (C) the difference in frequencies between duration (long flood – short flood). Positive numbers indicate greater dye coverage in the long duration for that depth and dye coverage.

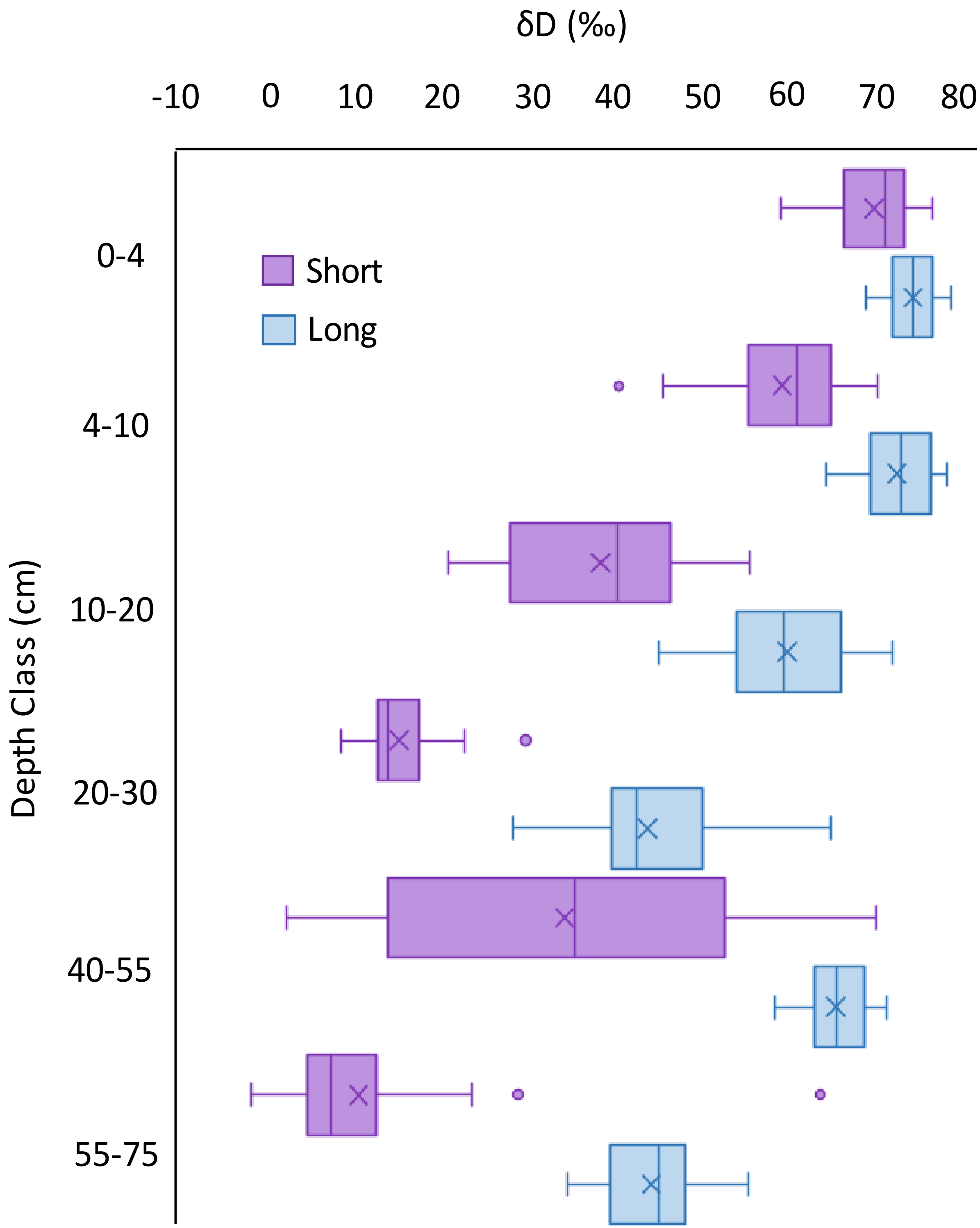

Figure 10. Boxplots of treatment ped δD separated by duration and depth class.

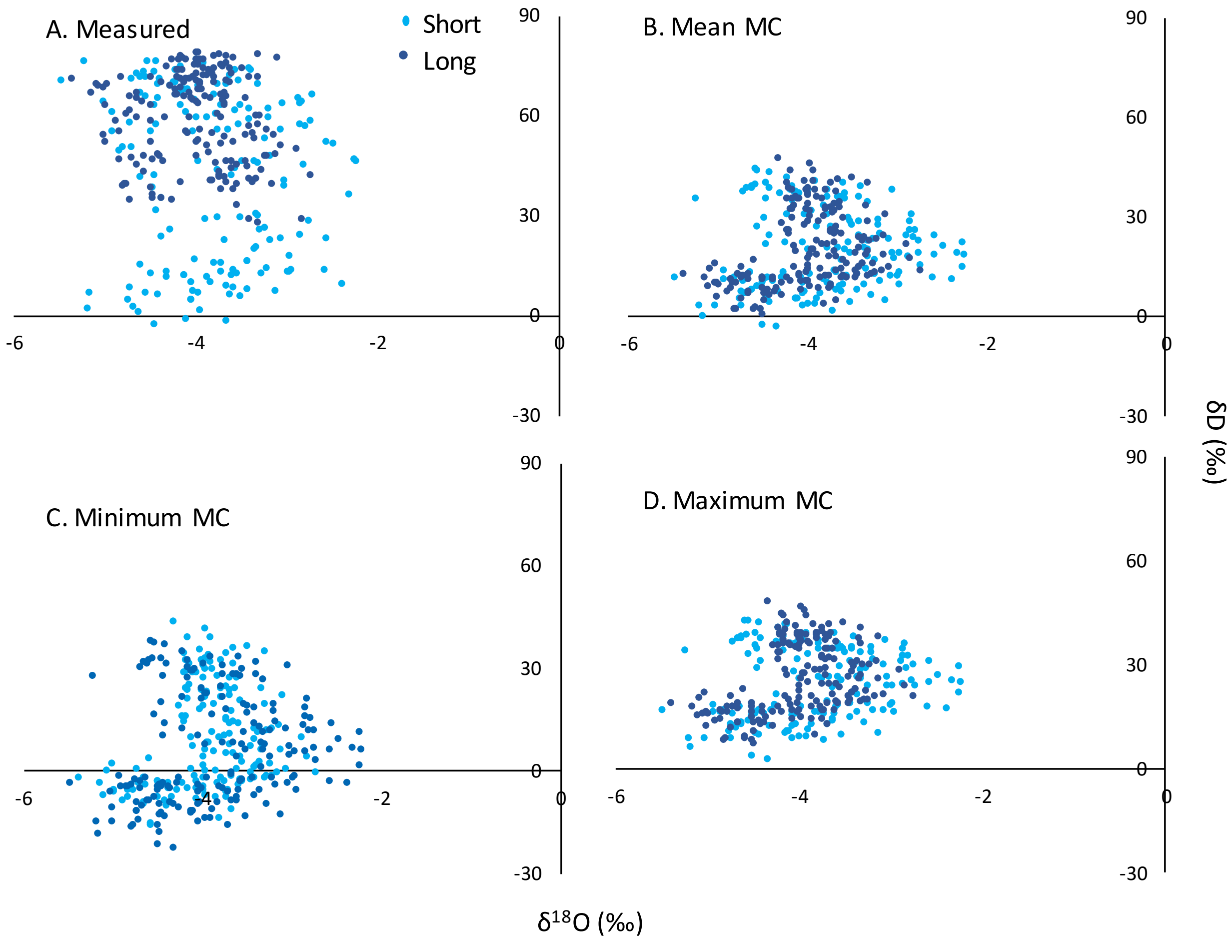

Figure 11. $\delta^{18}O$ and δD for measured peds (A) and expected $\overline{x}$ (B), minimum (C), and maximum (D) δD. All $\delta^{18}O$ reported are measured for each ped. Expected values were calculated using estimated initial control ped δD and moisture content (MC). Expected is a mixing ratio of pretreatment water and spiked treatment water calculated by change in moisture content from field to post treatment.

Much of the variance in δD was related to organic matter. There was a significant relationship between percent organic matter and δD in ped water for both short and long treatments. For peds with percent organic matter content up to approximately 9%, δD increased with percent organic matter (Fig. 13), but with high variance. After approximately 9% organic matter, the relationship varied little and almost all peds were dominated by flood water.

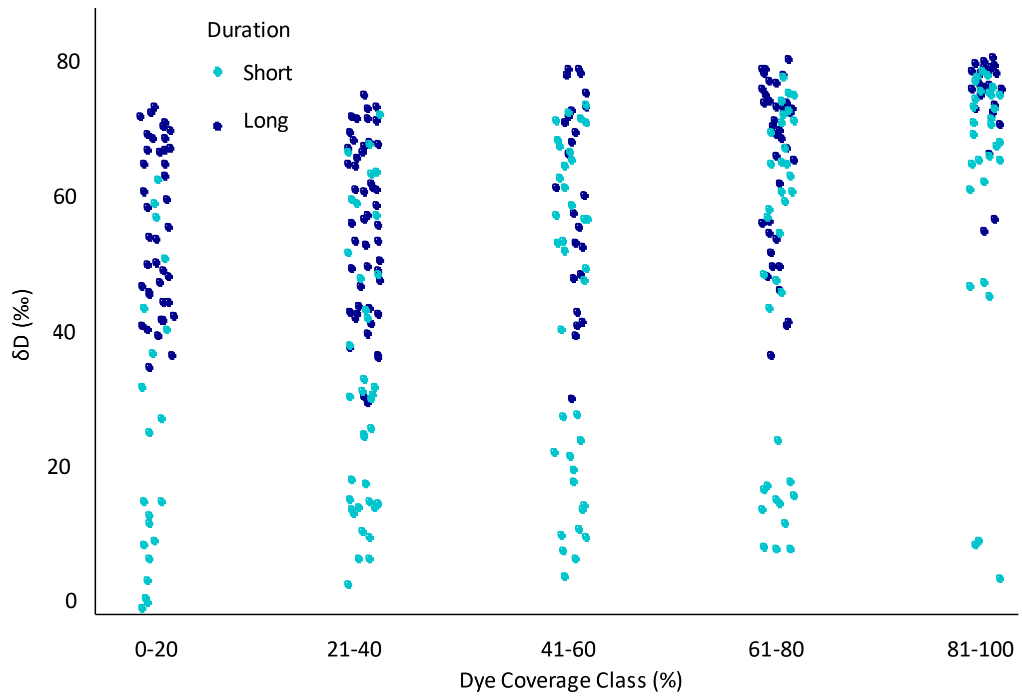

Figure 12. Ped percent dye coverage by δD. Horizontal variation within dye classes is jitter to separate each data point for visualization

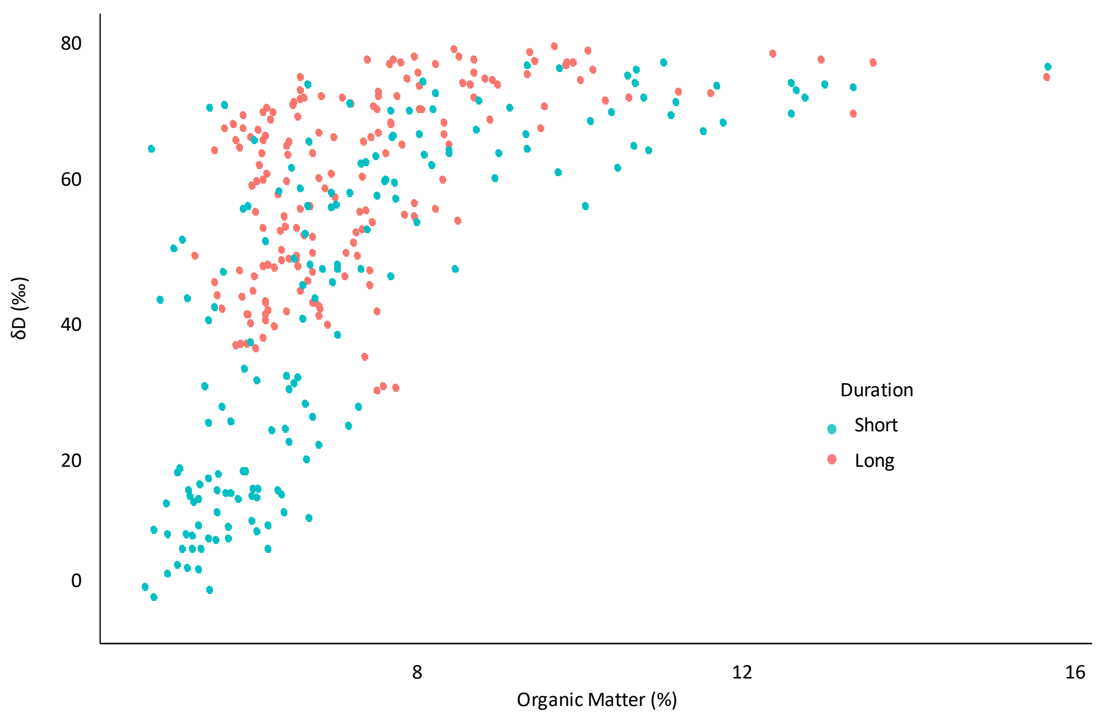

Figure 13. Scatterplot of δD values by percent organic matter for both treatment durations.

When plotted in dual isotope space, both $\delta^{18}O$ and δD decrease with depth, although $\delta^{18}O$ has much smaller range than deuterium (δD= -5 to +80 ‰ and $\delta^{18}O$= -2 to -6‰; Fig. 14). This is expected because no ^{18}O tracer was used in the treatment and the $\delta^{18}O$ of the tank tap water ($\delta^{18}O$= -5‰) fell within the range of the initial soil water $\delta^{18}O$ ($\delta^{18}O$= -0 to -5‰). The trend of decreasing $\delta^{18}O$ and δD with depth in the field samples was consistent with evaporation fractionation *in situ*.

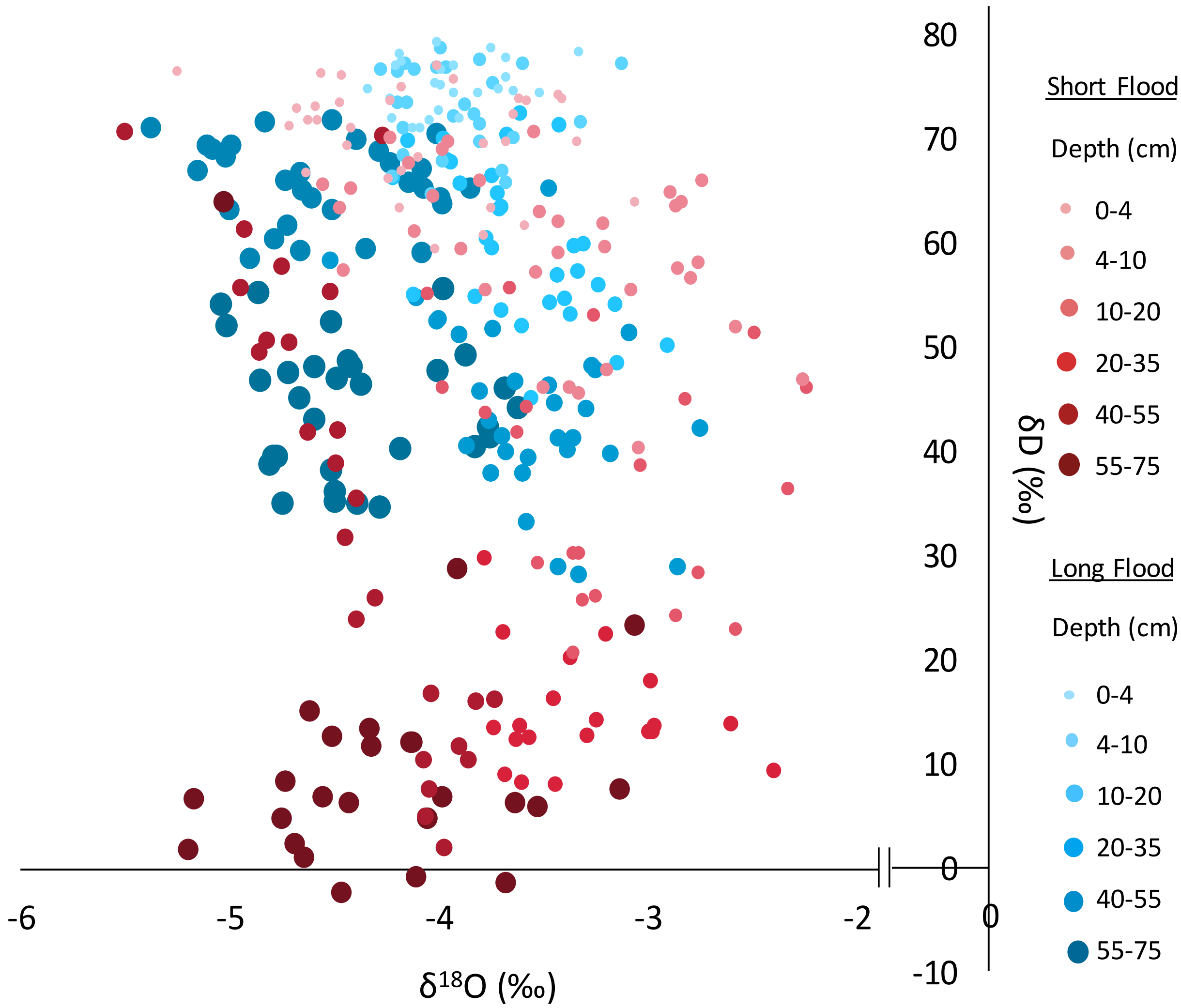

Figure 14. Dual isotopes for all treatment peds colored by duration and sized by depth class.

In both treatment durations, peds with the highest percent of organic matter occupy the same space, similar to flood water $\delta^{18}O$ and δD (Fig. 15). A pattern of increasing δD with increased percent organic matter can be seen when plotted in dual isotope space for both artificial flood durations and controls. There is no distinct pattern of organic matter effects on $\delta^{18}O$ in the flooded peds, which is expected as the flood water falls within the range of the control ped $\delta^{18}O$ water. However, the $\delta^{18}O$ in the control peds increase with increasing organic matter. This is likely due to evaporative fractionation in the surface peds and organic matter being higher at the surface.

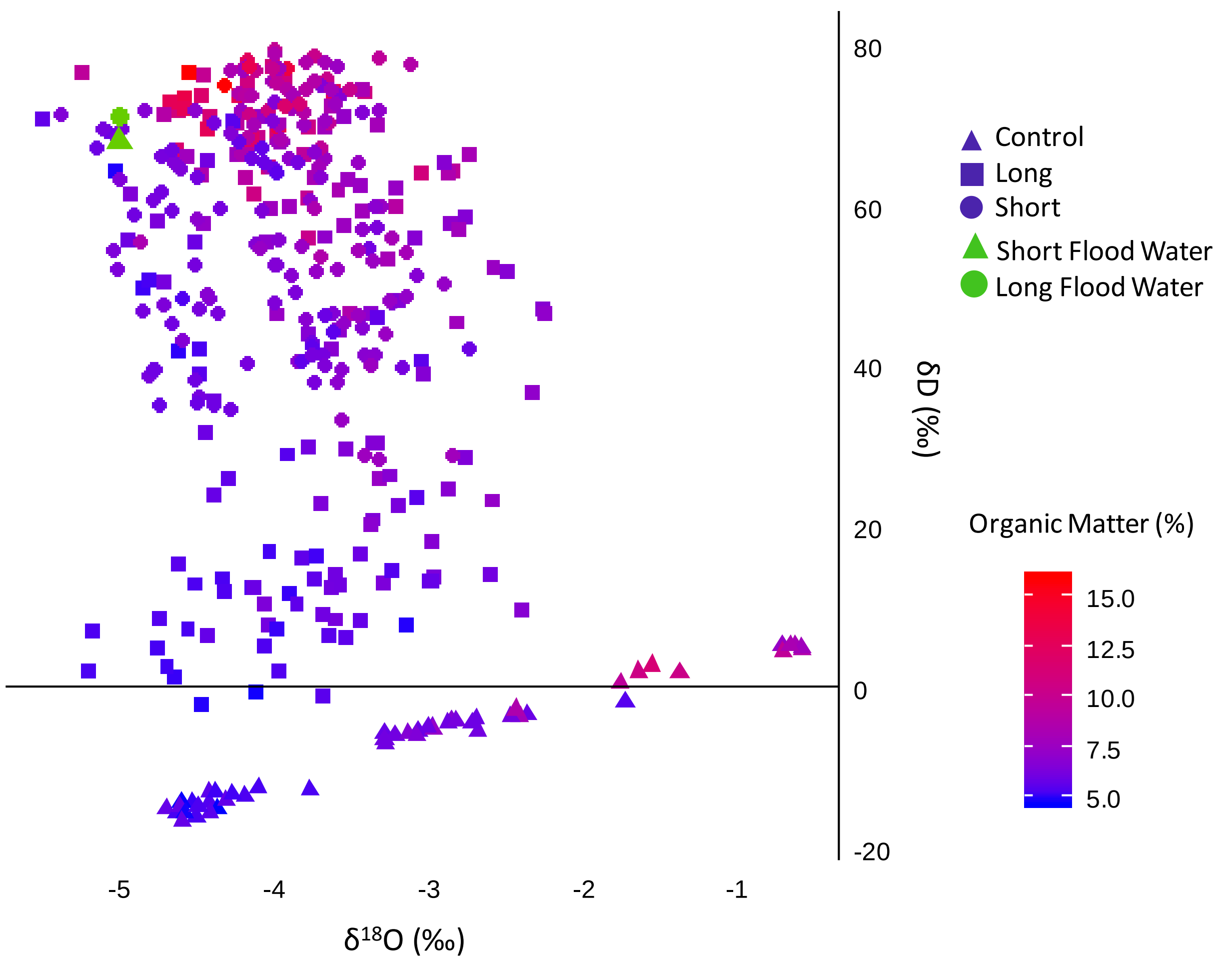

Figure 15. δD and $\delta^{18}O$ for tank flood water, control ped water, and flooded ped water. Color corresponds to percent organic matter.

DISCUSSION

Results from this experiment indicate matrix recharge in shrink-swell forest soil is a two-step process involving rapid mass flux via macropores into peds during the initial wet-up, followed by a period of slower increases in moisture content. The relatively steady moisture content and lack of greater macropore connectivity (dye staining) between the short and long durations suggest mass water flux ceased relatively quickly after flooding, likely within a few hours. The subsequent increase in δD indicates that flux after initial wet-up was dominated by diffusional processes.

Combining dye with stable isotopes allowed flow type to be distinguished between macropore and matrix flow. Dye coverage of peds tells a similar story as the moisture content and δD data. Deuterium, however, is better for identifying matrix water flux because it is relatively non-sorbing. Differences in tracer behaviors supported inferences of dominant flow mechanisms. For example, a greater proportion of peds with little to no dye coverage ($\leq$ 20%) and high δD in the 40-55 cm depth class suggest diffusional water movement was substantial and also dominated over macropore flux for this depth class. Dye coverage at this depth did not increase over time, but δD equilibrated to the spiked tank water and was similar to depth class 0-4 cm in concentration and variation.

Soil organic matter is an important control on soil water flux, as indicated by isotopes and moisture content changes during the experiment. Organic matter increases both water-holding capacity and macropore connectivity (Brady and Weil, 1999). It is hard to separate related variables such as organic matter, soil structure, and macropore connectivity, all of which are related to depth, in heterogeneous field soils, but the experimental design and tank set up allowed the effects of clay swelling and structure on flow mechanisms to be separated from the effects of organic matter on flow mechanisms. The top 10-15 cm depths of both monoliths in each tank (0-4 and 4-10 cm depth classes combined and 40-55 cm) had nearly equal opportunity to expand upon wetting, but differed in organic matter. The trend of decreasing deuterium at increasing depth was interrupted at depth 40-55 cm; likely due to the release of surrounding pressure and ability to expand due to the discontinuities in the monoliths at that depth. The large range in δD during the short artificial flood for this depth class is likely due to swelling over time. In the long artificial flood duration δD had much less variability in the 40-55 cm depth class, but was still at lower concentrations than depths 0-4 and 4-10 cm. Depth classes 0-4 and 4-10 cm had many more fine roots present in the soil than any other depth classes. Obtaining structured peds was more difficult here than at depth due to high organic matter present. Soil aggregates were smaller at the surface and discarded soil from the top 10 cm was much "grainier", more dyed, and less structured than the soil from deeper depths.

Dye tracers and rapid response of soil water deuterium indicate that macropore connectivity was responsible for water flow during the initial wet-up period, but did not dominate during the subsequent period (3 to 31 days). The surface crack network was visible before the monoliths were dunked, but was not visible after both flood durations. If the macropore network were still active during extended flood times, greater dye coverage would be expected in the long duration than the short. However, depth class of 20-35 cm was the only depth class with any significant difference in macropore connectivity between flood durations, with the short flood duration having greater macropore connectivity. This experiment was unable to resolve the exact timing of crack closure and macropore deactivation. However, results are consistent with Favre et al. (1997), who used a pin system to measure the rate of crack closure on a Vertisol soil in the field, and found that after just 4.5 hours surface cracks had closed despite lack of satiation in the soil matrix, but even after the 24 hour experimental period macropore cracks had not completely closed at greater depths.

The relatively small increase in soil moisture at depth, the fact that moisture content was lower at depth than at the surface (episaturation), and the relatively constant moisture content after one month of inundation were surprising: these data illustrate how slow water flux is into these soils after an initial wet-up occurs.

Our results, combined with reports from field studies, give a consistent picture of the hydrology of Vertisols in forested floodplains. Similar steady moisture contents over time have been found in other Vertisols. Miller and Bragg (2007) found top-down, episaturation of field soil, with moisture content variation with depth, similar to that of our experiment, in a forested Vertisol in Brazoria County, Texas. They reported that, during ponded conditions, ped interiors were wet (≥50% gravimetric soil water content and soil glistened) down to 30 cm during the first two weeks of ponding and down to 50 cm after 3 weeks. They also found relatively small differences in gravimetric moisture content between soil under extended ponding and soil from prolonged seasonally dry conditions at 100 cm. The most obvious difference between the Texas soil and the soil for this study is that the Texas soil had greater changes over time in the upper 50 cm. Similarly, Slabaugh (2006) found relatively consistent soil moisture with little apparent response to precipitation from depths of 25 cm, 50 cm, 100 cm, and 200 cm for two Vertisols in Mississippi over a 6-month period. They also found subsoil moisture content varied by only ± 4% annually, similar to the 3% increase found between the short and long artificial flood durations found in this experiment. Pettry and Switzer (1996) reported consistent soil moisture contents despite precipitation patterns in four Mississippi Sharkey soils over a 5-year period. They found the upper 50 cm had the highest moisture contents and was responsible for 80% of the total variation in moisture contents across all four sites. Although this experiment did not sample soil to depths below 75 cm, the study soil had similar behavior of little to no change in moisture content over time under flooded conditions from depths of 4-75 cm, excluding the depth class of 40-55 cm which is likely because the experimental set-up allowing more swelling than the other depth classes. Episaturation may be happening even if the intermediate layers are “saturated” be constriction rather than satiation; the concept of saturation is problematic for vertic clays.

Our experimental data and the results of field investigations of Vertisols indicate that distinct water pool partitioning, such as described by the “two water worlds” hypothesis, in floodplain Vertisols is not likely in the upper 10-50 cm because surface soils are typically responsive to precipitation (Pettry and Switzer, 1996; Slabaugh, 2006; Miller and Bragg, 2007). Matrix recharge occurs fairly quickly in surface depths after precipitation or flood events. The δD in the upper profile should be expected to reflect local precipitation events and evidence of evaporative fractionation. In this experiment, after only three days of flooding, the δD of soil water in the upper 10 cm closely matched the flood water. Below 10 cm all soil had additions of flood water, but the effect decreased with increasing depth. Farrish, (1991) concluded from three forested sites in Louisiana that approximately 60 to 64% of the fine-root biomass exist in the top 20 cm of soil and biomass decreases abruptly with depth. If the fine roots are concentrated in the soil that is most responsive to precipitation and flooding events, and soil and event water at these depths quickly mix, it is likely the trees would return water closely resembling a mix of the latest event water.

Given relatively constant soil moisture, non-responsiveness to precipitation events, and episaturation in Vertisols at < 50 cm below the surface, the possibility for TWW to exist in this system cannot be ruled out. In the case of episaturation where deeper soil profiles are not saturated and swelling of upper soil horizons prevents downward saturation, the bulk soil water of dryer deeper depths would likely be distinct from saturated shallower soil as hydrologic disconnection would prevent diffusional processes from occur. Under these conditions it would be possible for tree and stream water to occupy different areas when plotted in dual isotopic space, as the tree water would be a mix of bulk soil water, and the stream water would primarily come from unmixed bypass and overland flow from local precipitation events, and not from translatory flow processes. If deeper depths remain saturated and moisture contents fluctuate very little seasonally, evidence from the long artificial flood duration suggest that over time bulk soil water equilibrates with more mobile water pools. This is likely the case during prolonged flood conditions when the soil profile is saturated throughout, and isotopic diffusion and equilibration can readily occur, here we would not expect TWW to hold. TWW is an example of why more experiments explicitly examining soil water recharge and release are needed to better understand watershed hydrology in these vertic floodplain systems.

CONCLUSIONS

Macropore activity decreases with depth, and combined with organic matter controls mass flux into soil peds. The combined influence of these variables is expressed in depth below the surface. Macropores are active and dominate during the initial wet-up period, but close relatively quickly resulting in diffusional processes recharging the matrix beyond initial wet-up. This interruption of macropore connectivity explains field observations of steady soil moisture, episaturation, and lack of connectivity between surface ponding and subsurface water pools in Vertisols.

LITERATURE CITED

Allen, J. B. and H. J. Braud, Jr. 1966. Effect of cracks and initial moisture content on the infiltration rate of Sharkey clay. LSU Agricultural Experimental Station Reports. 823.

Allen, S. T. and R. F. Keim. 2017. Wetland-tree growth responses to hydrologic variability derived fromdevelopment and optimization of a non-linear radial growth model. Ecological Modelling 354: 49-61.

Arriaga, F. J., B. Lowery, and M. D. Mays. 2006. A fast method for determining soil particle size distribution using a laser instrument. Soil Science 171: 663-674.

Aslan, A. and W. J. Autin. 1999. Evolution of the Holocene Mississippi River floodplain, Ferriday, Louisiana: Insights on the origin of fine-grained floodplains. Journal of Sedimentary Research 69: 800-815.

Behera, U. K., A. R. Sharma, H. N. Pandey. 2007. Sustaining productivity of wheat-soybean cropping systems through intergrated nutrient management practices on the Vertisols of central India. Plant Soil 297: 185-199.

Berry, Z. C., J. Evaristo, G. Moore, M. Poca, K. Steppe, L. Verrot, H. Asbjornsen, L. S. Borma, M. Bretfeld, P. Hervé-Fernández, M. Seyfried, L. Schwenenmann, K. Sinacore, L. D. Wispelaere. J. McDonnell. 2016. The two water worlds hypothesis: Addressing multiple working hypotheses and proposing a way forward. Ecohydrology 11: e1843.

Beuselinck, L., G. Govers, J. Poesen, G. Degraer, and L. Froyen. 1998. Grain-size analysis by laser diffractometry: comparison with the sieve-pipette method. Catena 32: 193-208.

Beven, K. and P. Germann. 1982. Macropores and water flow in soils. Water Resources Research 18: 1311-1325.

Brady, N. C. and R. R. Weil. 1999. The Nature and Properties of Soils. Prentice-Hall. Upper Saddle River, New Jersey, United States.

Broadfoot, W. M. 1962. The fame of Sharkey clay. Forests and People 12: 30-31.

Broadfoot, W. M. and H. L. Williston. 1973. Flooding effects on southern forests. Journal of Forestry 71: 584-587.

Brooks, J. R., H. R. Barnard, R. Coulombe, and J. J. McDonnell. 2010. Ecohydrologic separation of water between trees and streams in a Mediterranean climate. Nature GeoScience 3: 100-104.

Das Gupta, S., B. P. Mohanty, and J. M. Köhne. 2006. Soil hydraulic conductivities and their spatial and temporal variations in a Vertisol. Soil Science Society of America Journal 70: 1872-1881.

De Jager, N. R., M. Thomsen, and Y. Yin. 2012. Threshold effects of flood duration on the vegetation and soils of the Upper Mississippi River floodplain, USA. Forest Ecology and Management 270: 135-146.

Doble, R. C., R. S. Crosbie, B. D. Smerdon, L. Peeters, and F. J. Cook. 2012. Groundwater recharge from overbank floods. Water Resource Research 48: W09522.

Eshel, G., G. J. Levy, U. Mingelgrin, and M. J. Singer. 2004. Critical evaluation of the use of laser diffraction for particle-size distribution analysis. Soil Science Society of America Journal 68: 736-743.

Evaristo, J., S. Jasechko, and J. J. McDonnell. 2016. Global separation of plant transpiration from groundwater and streamflow. Nature 525: 91-94.

Farrish, K. W. 1991. Spatial and temporal fine-root distribution in three Louisiana forest soils. Soil Science Society of America Journal 55: 1752-1757.

Favre, F., P. Boivin, and M. C. S. Wopereis. 1997. Water movement and soil swelling in a dry, cracked Vertisol. Geoderma 78: 113-123.

Flury, M., H. Flühler, W. A. Jury, and J. Leuenberger. 1994. Susceptibility of soils to preferential flow of water: A field study. Water Resources Research 30.7: 1945-1954.

Flury, M. and H. Fluhler. 1995. Tracer characteristics of Brilliant Blue FCF. Soil Science Society of America 59.1: 22-27.

Freebairn, D. M., L. D. Ward, A. L., Clarke, and G. F. Smith. 1986. Research and development of reduced tillage systems for Vertisols in Queensland, Australia. Soil and Tillage Research 8: 211-229.

Fynn, R. W. S., and M. Murray-Hudson. 2015. African wetlands and their seasonal use by wild and domestic herbivores. Wetlands Ecology and Management 23: 559-581.

Garvelmann, J, C. Külls, and M. Weiler. 2012. A porewater-based stable isotope approach for the investigation of subsurface hydrological processes. Hydrology and Earth System Sciences 16: 631-640.

Gat, J. R. 1966. Oxygen and hydrogen isotopes in the hydrologic cycle. Annual Review of Earth Planet Science 24: 225-262.

Geris, J., D. Tetzlaff, J. J. McDonnell, and C. Soulsby. 2017. Spatial and temporal patterns of soil water storage and vegetation water use in humid northern catchments. Science of the Total Environment 595: 486-493.

Goldsmith, G. R., L. E. Muñoz-Villers, F. Holwerda. J. J. McDonnell, H. Asbjornsen, and T. E. Dawson. 2012. Stable isotopes reveal linkages among ecohydrological processes in a seasonally sry tropical montane cloud forest. Ecohydrology 5: 779-790.

Gralher, B., B. Herbstritt, M. Weiler, L. I. Wassenaar, and C. Stumpp. 2018. Correcting for biogenic gas matrix effects on laser-based pore water-vapor stable isotope measurements. Vadose Zone Journal 17:170157.

Hardie, M., R. Doyle, W. Cotching, G. Holz, and S. Lisson. 2013. Hydropedology and preferential flow in the Tasmanian texture-contrast soils. Vadose Zone Journal 12:4.

Hester, E. T., C. R. Guth, D. T. Scott, and C. N. Jones. 2016. Vertical surface water-groundwater exchange processes within a headwater floodplain induced by experimental floods. Hydrological Processes 30: 3770-3787.

Hewlett, J. D. and A. R. Hibbert. 1967. Factors affecting the response of small watersheds to precipitation in humid areas. Forest hydrology: 275-290.

Hillel, D. 1998. Environmental Soil Physics. Academic Press, London, UK.

Hook, D. D. 1984. Waterlogging tolerance of lowland tree species of the south. Southern Journal of Applied Forestry 8: 136-149.

Howard, P. J. A. 1965. The carbon-organic matter factor in various soil types. Oikos 15.2: 229-236.

Hunter, R. G., S. P. Faulkner, and K. A. Gibson. 2008. The importance of hydrology in restoration of bottomland hardwood wetland functions. Wetlands 28: 605-615.

Jena, R. K., R. Jagadeeswaran, and R. Sivasamy. 2013. Analogy of soil parameters in Particle Size Analysis through Laser Diffraction Techniques. Indian Journal of Hill Farming 26: 78-83.

Jones, L. D. and I. Jefferson. 2012. Expansive Soils. Pages 413-441 in J. Burland, T. Chapman, H. D. Skinner, and M. Brown, editors. ICE manual of geotechnical engineering volume 2: Geotechnical design, construction, and verification. ICE Publishing, London, United Kingdom.

Jung, M. and T. P. Burt. 2004. Toward a conceptual model of floodplain water table response. Water Resources Research 40: W12409.

Kendall, C. and J. J. McDonnell. 1998. Isotope tracers in catchment hydrology. Elsevier, Amsterdam, the Netherlands.

Ketelsen, H. and S. Meyer-Windel. 1999. Adsorption of brilliant blue FCF by soils. Geoderma 90: 131-145.

King, S. L. and B. D. Keeland. 1999. Evaluation of reforestation in the Lower Mississippi River Alluvial Valley. Society for Ecological Restoration 7.4: 348-359.

King, S. L. and R. F. Keim. 2019. Hydrologic modifications challenge bottomland hardwood forest management. Journal of Forestry.

Klute, A., editor. 1986. Soil Science Society of America Book Series: 5. Methods of Soil Analysis Part 1- Physical and Mineralogical Methods. Second Edition. American Society of Agronomy, Inc. and Soil Science Society of America, Inc., Madison, Wisconsin USA.

Knapp, A. K., C. E. Burns, R. W. S. Fynn, K. P. Kirkmann, C. D. Morris, and M. D. Smith. 2006. Convergence and contingency in production–precipitation relationships in North American and South African C_4 grasslands. Oecologia 149: 456-464.

Kroschel, W. A., S. L. King, and R. F. Keim. 2016. Tree regeneration by seed in bottomland hardwood forests: a review. Southeastern Naturalist 15(Special Issue): 42-60.

Krzywicka, A. E., G. E. Pociask, D. A. Grimley, J. W. Matthews. 2017. Hydrology and soil magnetic susceptibility as predictors of planted tree survival in a restored floodplain forest. Ecological Engineering 109: 275-287.

Lal, R. 1987. Managing the soils of Sub-Saharan Africa. Science 236: 1069-1076.

Lin, Y. and J. Horita. 2016. An experimental study on isotope fractionation in a mesoporous silica-water system with implications for vadose-zone hydrology. Geochimica et Cosmochimica Acta 184: 257-271.

Lin, Y., J. Horita, and O. Abe. 2018. Adsorption isotope effects of water on mesoporous silica and alumina with implications for the land-vegetation-atmosphere system. Geochimaca et Cosmochimica Acta 223: 520-536.

Marshall, T. J., J. W. Holmes, and C. W. Rose. 1996. Soil Physics: Third Edition. Cambridge University Press. Cambridge, UK.

Majoube, M. 19741. Fractionation of oxygen 8 and deuterium between water and its vapor (In French). Journal de Chimie Physique et de Physico-Chimie Biologique 68: 1423-1436.

Miller, W. L. and A. L. Bragg. 2007. Soil Characterization and Hydrological Monitoring Project, Brazoria County, Texas, Bottomland Hardwood Vertisols. United States Department of Agriculture, Natural Resources Conservation Service, Temple, Texas.

NCSS. 2013. Sharkey series. National Cooperative Soil Survey, U.S.A.

NRCS. Web soil survey. Accessed 10/20/2017. <https://websoilsurvey.sc.egov.usda.gov/App/WebSoilSurvey.aspx>.

Natural Resource Conservation Service (NRCS). 1992. Primary Characterization Data, Iberville Parish, Louisiana. Lincoln, Nebraska, USA. <https://ncsslabdatamart.sc.egov.usda.gov/rptExecute.aspx?p=15532&r=1&submit1=Get+Report>

Oerter, E., K. Finstad, J. Schaefer, G. R. Goldsmith, T. Dawson, R. Amundson. 2014. Oxygen isotope fractionation effects in soil water via interaction with cations (Mg, Ca, K, Na) adsorbed to phyllosilicate clay minerals. Journal of Hydrology 515: 1-9.

Öhrstrom, P., Y. Hamed, M. Persson, and R. Berndtsson. 2004. Characterizing unsaturated solute transport by simultaneous use of dye and bromine. Journal of Hydrology 289: 23-35.

Özer, M., M. Orhan, and N. S. Işik. 2010. Effect of particle optical properties on size distribution of soils obtained by laser diffraction. Environmental & Engineering Geoscience 16: 163-173.

Pettry, D. E. and R. E. Switzer. 1996. Sharkey soils in Mississippi. Division of Agriculture, Forestry, and Veterinary Medicine, Mississippi State University. Starkville, Mississippi.

Rawls, W. J., Y. A. Pachepsky, J. C. Ritchie, T. M. Sobecki, and H. Bloodworth. 2003. Effect of soil carbon on soil water retention. Geoderma 116: 61-76.

Ritchie, J. T., D. E. Kissel, E. Burnett. 1972. Water movement in undisturbed swelling clay soil. Soil Science Society of America 36: 874-879.

Romkens, M. J. M. and S. N. Prasad. 2006. Rain infiltration into swelling/shrinking/cracking soils. Agricultural Water Management 86: 196-205.

Saxton, K. E. and W. J. Rawls. 2006. Soil water characteristic estimates by texture and organic matter for hydrologic solutions. Soil Science Society of America Journal 70: 1569-1578.

Skiadaresis, G., J. A. Schwarz and J. Bauhus. 2019. Groundwater extraction in floodplain forests reduces radial growth and increases summer drought sensitivity of Pedunculate Oak trees (*Quercus robar* L.). Frontiers in Forests and Global Change 2:5.

Slabaugh, J. D. 2006. Final report: study of Sharkey Soils in the Lower Mississippi Valley. United States Department of Agriculture, Natural Resources Conservation Service, Little Rock, Arkansas.

Stewart, R. D., M. R. A. Najm, D. E. Rupp, and J. S. Selker. 2016. Modeling multidomain hydraulic properties of shrink-swell soils. Water Resources Research 52: 7911-7930.

Taylor, J. R., Cardamone, M. A., & Mitsch, W. J. (1990). Bottomland hardwood forests: their functions and values. Ecological processes and cumulative impacts illustrated by bottomland hardwood wetland ecosystems. Lewis Publ., Chelsea, MI, 13-86.

United States Department of Agriculture (USDA) and Natural Resources Conservation Service (NRCS). 1999. Soil taxonomy: A basic system for soil classification for making and interpreting soil surveys. Second Edition. Washington, DC, US.

Walbridge, M. R. 1993. Functions and values of forested wetlands in the southern United States. Journal of Forestry 91: 15-19.

Wassenaar, L. I., M. J. Hendry, V. L. Chostner, and G. P. Lis. 2008. High resolution pore water δ^2H and $\delta^{18}O$ measurements by $H_2O_{(liquid)}$-$H_2O_{(vapor)}$ equilibration laser spectroscopy. Environmental Science and Technology 42.24: 9262-9267.

Weiler, M. and H. Flühler. 2004. Inferring flow types from dye patterns in macroporous soils. Geoderma 120.1: 137-153.

APPENDIX A. PHOTOS

Figure A.1. Sampling site in St. Gabriel, Louisiana. Back-hoe was used to dig a soil point of entry.

Figure A.2. Image of monolith excavation. The soil surrounding the sampled monolith was dug out to fit snugly in the small drums. The outer edges of soil were picked with a knife to remove smeared edges caused by large shovels.

Figure A.3. Soil face at 6 cm depth after excavation of shallower depths. The macropore network is clearly visible with the blue dye.

Figure A.4. Soil face at 10 cm depth taken from long duration monolith. Macropore network is still clearly and a medium root can be seen in the top right of the barrel.

Figure A.5. Soil face at 20 cm. Many fine roots are present and the macropore network is still very visible.


Figure A.6. Soil face of short duration monolith at 40 cm. Top half has exterior peds removed (approximately 2 cm) and the lower half is exposed non-excavated soil.

Figure A.7. Soil face at 40 cm from long duration with approximately outer 3 mm picked off. Fine roots less present while medium roots are dominate. A large macropore created by an active grub worm can be seen in top center of monolith.

Figure A.8. Large structural root can be seen in long duration monolith at a depth of 20 cm. This is the largest root found of all soil sampled.

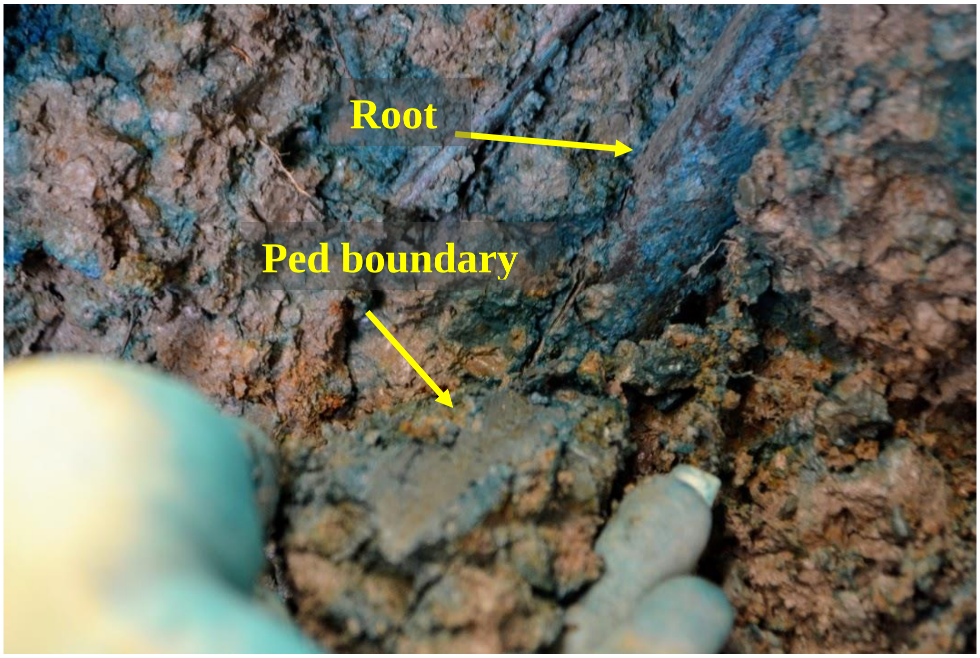

Figure A.9. Close-up of smooth ped boundary around large root.

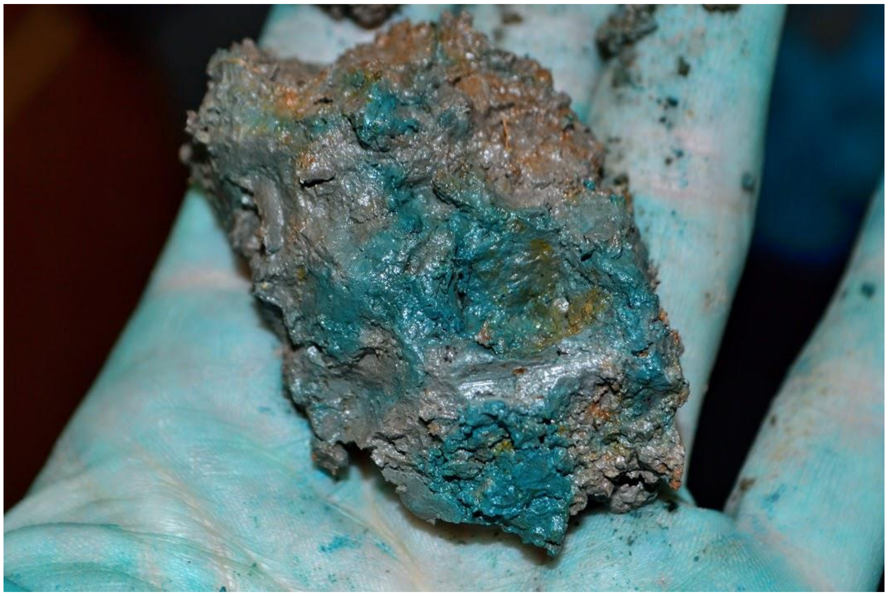

Figure A.10. Individual ped with smooth slickensides visible. Glossy appearance suggest saturation.

Figure A.11. Edge of long duration soil monolith at 75 cm depth. Only approximately 2-3 mm of dye penetrated into the soil from the edge.

APPENDIX B. DATA

Table B.1. Laser diffraction particle size analysis results using laser diffraction classifying particles sizes based on ≤2.0 µm cut-off for clay size. Values presented are percent of total by volume. Soil texture class is silty clay loam.

Depth	**Clay** ≤2 µm	**Silt** 2-50 µm	**Fine Sand** 50-200 µm	**Coarse Sand** ≥200 µm
0-4	38.03	57.57	8.34	1.01
4-10	41.35	58.39	3.47	0.12
10-20	37.73	61.41	0.86	0.00
20-35	37.19	61.75	1.06	0.00
40-55	39.05	60.95	0.00	0.00
55-75	42.76	56.80	0.43	0.00
Combined Average	**37.97**	**59.48**	**2.36**	**0.19**

Table B.2. Particle size analysis results using laser diffraction classifying particles sizes based on ≤2.99 µm cut-off for clay. Values presented are percent of total by volume. Soil texture class is silty clay.

Depth	**Clay** ≤2.99 µm	**Silt** 3-50.99 µm	**Fine Sand** 51-200.99 µm	**Coarse Sand** ≥201 µm
0-4	45.09	45.56	8.34	1.01
4-10	51.54	44.84	3.47	0.12
10-20	51.97	47.17	0.86	0.00
20-35	51.96	46.98	1.06	0.00
40-55	54.87	45.13	0.00	0.00
55-75	56.88	42.68	0.43	0.00
Combined Average	**52.05**	**45.40**	**2.36**	**0.19**

Table B.3. Particle size analysis results from 1992 NRCS Sharkey soil report.

*** Primary Characterization Data ***

Pedon ID: 88LA047002 (IbervilleParish, Louisiana) Print Date: Apr 1 2019 9:38AM

Sampled As : Sharkey Very-fine, montmorillonitic, nonacid, thermic Vertic Haplaquept

USDA-NRCS-NSSC-Soil Survey Laboratory ; Pedon No. 89P0047

PSDA & Rock Fragments				-1-	-2-	-3-	-4-	-5-	-6-	-7-	-8-	-9-	-10-	-11-	-12-	-13-	-14-	-15-	-16-	-17-	-18-
					(- - - - - Total - - - - - -)			(- - Clay - - -)		(- - - - Silt - - - - -)		(- - - - - - - - - - - - Sand - - - - - - - - - - - -)					(Rock Fragments (mm))				
				Lab	Clay	Silt	Sand	Fine	CO_3	Fine	Coarse	VF	F	M	C	VC	(- - - - - - - - Weight - - - - - - - -)				>2 mm
				Text-	<	.002	.05	<	<	.002	.02	.05	.10	.25	.5	1	2	5	20	.1-	wt %
	Depth			ure	.002	-.05	-2	.0002	.002	-.02	-.05	-.10	-.25	-.50	-1	-2	-5	-20	-75	75	whole
Layer	(cm)	Horz	Prep		(- % of <2mm Mineral Soil -)												(- - - - - - - % of <75mm - - - - - -)				soil
				3A1a1a	3A1a1a	3A1a1a	3A1a1a	3A1a1a		3A1a1a	3A1a1a	3A1a1a	3A1a1a	3A1a1a	3A1a1a	3A1a1a	3B1	3B1	3B1		
89P00530	0-13	Ap	S	sic	48.3	41.5	10.2	23.5		30.1	11.4	8.1	1.6	0.3	0.2	--	2	5	--	9	7
89P00531	13-30	A	S	sic	54.3	43.3	2.4	28.4		37.0	6.3	1.9	0.5	--	--	--	tr	--	--	1	--
89P00532	30-50	Bg1	S	c	68.8	29.2	2.0	33.3		26.8	2.4	1.7	0.3	--	tr	--	--	--	--	tr	--
89P00533	50-85	Bg2	S	c	63.6	33.8	2.6	26.7		30.5	3.3	2.1	0.5	--	--	--	--	--	--	1	--
89P00534	85-132	Bg3	S	c	66.4	29.6	4.0	29.3		25.9	3.7	3.1	0.7	0.2	--	--	--	--	--	1	--
89P00535	132-158	Bssg1	S	c	53.8	30.5	15.7	25.4		13.5	17.0	14.1	1.5	0.1	--	--	--	--	--	2	--
89P00536	158-180	Bssg2	S	c	46.2	38.2	15.6	23.1		17.2	21.0	14.2	1.3	0.1	--	--	--	--	--	1	--
89P00537	180-212	BCg	S	cl	35.8	40.5	23.7	16.2		16.7	23.8	21.9	1.8	--	--	--	--	--	--	2	--

Table B.4. Control ped data used for analysis including soil physical properties and isotopic composition.

Depth (cm)	Wet Weight	Oven Dry Weight	Gravimetric Water Content	Organic Matter Percent	$\delta^{18}O$	δD
0-4	32.54	25.21	0.29	8.13	-0.62	5.16
0-4	24.68	19.63	0.26	7.33	-0.71	5.15
0-4	36.98	27.83	0.33	9.55	-0.70	4.22
0-4	24.61	17.78	0.38	10.54	-1.64	1.86
0-4	23.29	17.57	0.33	8.67	-0.58	4.65
0-4	16.23	11.63	0.40	10.40	-1.37	1.75
0-4	30.49	22.23	0.37	9.47	-1.75	0.45
0-4	82.99	64.16	0.29	7.80	-0.58	4.88
0-4	30.95	23.68	0.31	8.31	-0.66	5.03
0-4	23.27	17.11	0.36	11.34	-1.55	2.63

(table B.4. cont'd)

Depth (cm)	Wet Weight	Oven Dry Weight	Gravimetric Water Content	Organic Matter Percent	$\delta^{18}O$	δD
0-45	11.83	8.64	0.37	6.48	-2.85	-4.23
0-45	11.13	7.85	0.42	6.68	-2.85	-4.23
0-45	9.25	6.54	0.41	5.84	-3.28	-5.80
0-45	2.79	1.85	0.51	5.47	-1.72	-2.03
0-45	13.96	9.8	0.42	6.12	-2.68	-5.50
0-45	4.43	3.1	0.43	5.96	-2.69	-4.08
0-45	6.51	4.55	0.43	6.24	-2.98	-5.04
0-45	16.44	11.88	0.38	5.88	-3.07	-5.49
0-45	10.12	7.06	0.43	6.04	-2.87	-4.61
0-45	6.49	4.51	0.44	7.32	-2.97	-5.25
0-45	10.85	7.76	0.40	6.08	-3.21	-6.19
0-45	3.65	2.58	0.41	5.89	-2.36	-3.47
0-45	41.22	29.8	0.38	7.98	-2.41	-3.65
0-45	26.07	19.09	0.37	6.64	-3.13	-5.78
0-45	3.45	2.42	0.43	6.18	-2.47	-3.63
0-45	11.57	8.28	0.40	5.98	-3.00	-5.09
0-45	7.25	5.19	0.40	5.95	-2.72	-4.46
0-45	11.86	8.64	0.37	8.52	-2.44	-2.84
0-45	7.95	5.71	0.39	6.09	-3.28	-6.61
0-45	20.68	15.19	0.36	6.26	-2.82	-4.35
0-45	13.08	8.98	0.46	6.06	-3.28	-7.02
0-45	33.63	24.29	0.38	6.51	-3.07	-6.02
50-75	14.61	9.39	0.56	5.37	-4.42	-14.42
50-75	14.07	9.85	0.43	4.70	-4.36	-15.32
50-75	18.42	12.57	0.47	5.25	-4.50	-16.28
50-75	37.49	26.08	0.44	5.26	-3.77	-12.91
50-75	12.32	8.63	0.43	5.57	-4.42	-13.04
50-75	22.95	16.04	0.43	4.82	-4.59	-14.48

(table B.4. cont’d)

Depth (cm)	Wet Weight	Oven Dry Weight	Gravimetric Water Content	Organic Matter Percent	δ^{18}O	δD
50-75	30.91	21.95	0.41	5.03	-4.53	-14.40
50-75	12.69	8.87	0.43	5.10	-4.38	-13.01
50-75	16.46	11.29	0.46	5.76	-4.70	-15.13
50-75	10.38	7.09	0.46	5.71	-4.31	-14.20
50-75	12.48	8.74	0.43	5.23	-4.10	-12.58
50-75	17.83	12.45	0.43	4.72	-4.60	-14.50
50-75	21.87	15.64	0.40	5.23	-4.63	-15.65
50-75	8.23	5.86	0.40	5.53	-4.41	-15.62
50-75	15.98	10.94	0.46	5.74	-4.61	-15.03
50-75	24.02	16.94	0.42	4.76	-4.58	-15.81
50-75	12.21	8.56	0.43	5.48	-4.19	-13.66
50-75	26.45	18.92	0.40	5.29	-4.19	-13.66
50-75	15.26	10.54	0.45	5.29	-4.49	-14.85
50-75	15.33	10.65	0.44	5.13	-4.27	-13.42
50-75	45.03	32.09	0.40	5.75	-4.59	-16.81

Table B.5. Short treatment duration ped data including physical properties and isotopic values.

Depth (cm)	Percent Dye Coverage	Wet Weight	Oven Dry Weight	Gravimetric Water Content	Organic Matter Percent	δ^{18}O	δD
0-4	81-100	13.09	7.51	0.74	12.74	-3.61	74.02
0-4	81-100	6.89	3.87	0.78	13.15	-4.23	73.68
0-4	81-100	15.2	8.86	0.72	10.71	-4.17	75.04
0-4	61-80	33.64	20.78	0.62	8.00	-3.33	69.86
0-4	81-100	11.14	6.6	0.69	10.97	-3.05	64.02

(table B.5. cont’d)

Depth (cm)	Percent Dye Coverage	Wet Weight	Oven Dry Weight	Gravimetric Water Content	Organic Matter Percent	δ^{18}O	δD
0-4	61-80	8.64	5.04	0.71	10.80	-3.41	73.98
0-4	81-100	28.35	16.73	0.69	11.15	-4.00	77.14
0-4	41-60	13.11	7.75	0.69	10.51	-3.78	69.57
0-4	81-100	20.6	12.12	0.70	11.64	-4.63	66.82
0-4	41-60	15.59	9.15	0.70	11.31	-4.42	71.07
0-4	81-100	7.21	4.13	0.75	10.82	-3.92	75.85
0-4	81-100	9.94	6.03	0.65	8.18	-3.42	74.26
0-4	61-80	12.02	7.31	0.64	7.77	-3.67	69.79
0-4	61-80	10.44	6.38	0.64	8.28	-3.58	61.76
0-4	61-80	10.14	6.07	0.67	6.75	-3.58	73.72
0-4	41-60	11.31	6.88	0.64	8.33	-3.64	72.39
0-4	41-60	26.46	16.25	0.63	8.83	-4.17	66.98
0-4	81-100	4.54	2.45	0.85	13.50	-4.58	73.26
0-4	61-80	4.05	2.68	0.51	8.19	-3.74	63.42
0-4	61-80	8.11	4.85	0.67	10.24	-4.10	68.32
0-4	61-80	15.7	9.58	0.64	9.86	-4.46	76.27
0-4	61-80	6.16	3.89	0.58	7.70	-4.02	59.52
0-4	81-100	5.83	3.99	0.46	7.80	-4.24	66.25
0-4	81-100	34.61	21.2	0.63	9.47	-5.25	76.54
0-4	81-100	11.35	6.18	0.84	15.91	-4.56	76.46
0-4	81-100	4.04	2.21	0.83	12.73	-4.43	69.51
0-4	61-80	7.09	4.21	0.68	9.11	-4.18	63.46
0-4	61-80	10.38	6.17	0.68	8.86	-4.71	71.31
0-4	81-100	12.63	7.28	0.73	11.82	-4.47	73.60
0-4	61-80	18.56	10.88	0.71	12.79	-4.67	72.91
0-4	81-100	11.46	6.63	0.73	12.90	-4.57	71.91

(table B.5. cont'd)

Depth (cm)	Percent Dye Coverage	Wet Weight	Oven Dry Weight	Gravimetric Water Content	Organic Matter Percent	δ^{18}O	δD
0-4	81-100	5.36	3.12	0.72	10.91	-4.62	71.79
0-4	81-100	5.8	3.53	0.64	9.85	-3.78	60.77
4-10	41-60	14.28	8.83	0.62	7.59	-3.52	63.23
4-10	21-40	41.31	26.93	0.53	7.27	-3.55	70.91
4-10	81-100	8.04	4.52	0.78	11.89	-4.15	68.02
4-10	21-40	8.84	5.53	0.60	7.40	-3.21	62.09
4-10	0-20	15.05	9.52	0.58	7.03	-2.86	57.79
4-10	41-60	23.66	15.14	0.56	6.57	-3.20	47.97
4-10	41-60	15.65	9.39	0.67	8.30	-3.96	70.00
4-10	41-60	17.54	10.64	0.65	9.47	-2.84	64.15
4-10	21-40	32.88	21.41	0.54	7.11	-2.26	47.12
4-10	21-40	26.3	17.08	0.54	6.66	-2.76	58.36
4-10	41-60	12.56	8.57	0.47	8.12	-2.74	66.29
4-10	41-60	9.33	5.98	0.56	7.48	-2.58	52.22
4-10	61-80	30.48	18.87	0.62	8.50	-2.87	63.89
4-10	61-80	40.25	24.4	0.65	10.19	-3.78	55.76
4-10	81-100	43.29	25.97	0.67	11.25	-3.98	69.24
4-10	61-80	15.28	9.46	0.62	7.82	-3.43	59.32
4-10	41-60	10.24	6.63	0.54	6.74	-3.08	55.81
4-10	21-40	36.91	23.68	0.56	7.47	-3.43	62.34
4-10	41-60	16.12	9.93	0.62	9.07	-3.21	59.88
4-10	61-80	12.43	7.88	0.58	7.83	-2.80	56.91
4-10	21-40	20.01	12.87	0.55	6.76	-2.89	65.21
4-10	21-40	7.6	4.48	0.70	9.45	-3.81	66.32
4-10	21-40	57.89	37.91	0.53	7.26	-4.46	57.70
4-10	81-100	10.24	6.44	0.59	7.72	-3.90	59.72
4-10	41-60	24.02	15.52	0.55	6.93	-3.37	46.41

(table B.5. cont’d)

Depth (cm)	Percent Dye Coverage	Wet Weight	Oven Dry Weight	Gravimetric Water Content	Organic Matter Percent	$\delta^{18}O$	δD
4-10	21-40	15.2	9.52	0.60	8.58	-3.50	46.42
4-10	41-60	4.16	2.33	0.79	10.58	-4.12	61.42
4-10	21-40	9.05	6.04	0.50	5.59	-3.05	40.63
4-10	61-80	24.28	15.29	0.59	7.79	-4.56	65.95
4-10	81-100	8.88	5.38	0.65	9.25	-4.24	70.31
4-10	40-60	7.71	4.95	0.56	6.09	-4.42	65.41
4-10	41-60	6.46	3.97	0.63	7.61	-3.54	57.36
4-10	81-100	16.96	10.3	0.65	10.78	-4.03	64.66
4-10	81-100	18.4	12.35	0.49	5.70	-3.33	45.87
4-10	81-100	16.3	9.98	0.63	8.50	-4.47	63.58
10-20	61-80	9.97	6.23	0.60	8.10	-3.26	53.31
10-20	81-100	7.94	4.95	0.60	7.78	-2.82	45.32
10-20	61-80	10.72	6.86	0.56	7.05	-3.58	44.42
10-20	41-60	10.31	6.55	0.57	6.72	-2.49	51.69
10-20	61-80	33.87	22.45	0.51	6.78	-2.26	47.12
10-20	21-40	12.47	8.07	0.55	7.11	-2.24	46.45
10-20	21-40	18.04	11.71	0.54	6.81	-2.87	24.49
10-20	0-20	19.84	12.95	0.53	6.69	-3.04	38.94
10-20	21-40	21.65	13.82	0.57	7.10	-3.67	56.00
10-20	21-40	21.64	13.95	0.55	6.52	-2.76	28.59
10-20	21-40	14.64	9.46	0.55	7.25	-2.58	23.17
10-20	21-40	16.87	10.88	0.55	7.12	-2.33	36.64
10-20	61-80	22.95	14.71	0.56	7.41	-3.99	46.36
10-20	41-60	12.48	7.99	0.56	7.37	-3.32	26.02
10-20	81-100	7.93	5.06	0.57	6.69	-3.78	43.96
10-20	41-60	10.11	6.61	0.53	6.72	-3.25	26.30
10-20	41-60	8.78	5.53	0.59	7.04	-4.05	55.43

(table B.5. cont'd)

Depth (cm)	Percent Dye Coverage	Wet Weight	Oven Dry Weight	Gravimetric Water Content	Organic Matter Percent	$\delta^{18}O$	δD
10-20	61-80	18.91	12.37	0.53	6.83	-3.63	42.08
10-20	41-60	32.66	21.71	0.50	6.52	-3.36	20.83
10-20	21-40	13.41	8.56	0.57	6.49	-3.36	30.44
10-20	0-20	9.53	5.97	0.60	6.63	-3.33	30.40
10-20	21-40	21.7	14.01	0.55	6.57	-3.53	29.44
20-35	41-60	15.43	10.09	0.53	6.76	-2.39	9.44
20-35	21-40	44.88	29.24	0.53	6.13	-2.60	13.85
20-35	41-60	9.89	6.15	0.61	6.73	-2.98	18.11
20-35	21-40	26.05	17.19	0.52	6.38	-2.97	13.66
20-35	41-60	13.1	8.44	0.55	6.47	-3.69	22.68
20-35	61-80	9.59	6.29	0.52	6.30	-3.20	22.58
20-35	41-60	20.17	13.14	0.54	6.25	-3.60	8.33
20-35	21-40	27.99	18.05	0.55	6.05	-3.68	9.01
20-35	41-60	26.37	17.63	0.50	6.12	-3.63	12.45
20-35	0-20	30.13	19.91	0.51	5.62	-3.73	13.52
20-35	21-40	13.72	9.03	0.52	6.12	-3.78	29.78
20-35	61-80	26.01	16.87	0.54	5.98	-3.45	16.41
20-35	41-60	32.15	20.86	0.54	5.94	-3.45	16.41
20-35	41-60	56.65	38.08	0.49	6.42	-3.29	12.90
20-35	61-80	19.2	12.47	0.54	5.73	-2.99	13.18
20-35	21-40	21.3	14.17	0.50	5.77	-3.44	8.18
20-35	41-60	13.7	9.04	0.52	6.89	-3.37	20.29
20-35	21-40	12.14	7.85	0.55	5.80	-2.98	13.10
20-35	61-80	11.99	7.78	0.54	5.41	-3.24	14.37
20-35	21-40	13.69	8.9	0.54	6.06	-3.57	12.63
20-35	61-80	33.79	22.32	0.51	6.07	-3.61	13.82
40-55	0-20	10.3	6.48	0.59	5.08	-4.85	49.52

(table B.5. cont'd)

Depth (cm)	Percent Dye Coverage	Wet Weight	Oven Dry Weight	Gravimetric Water Content	Organic Matter Percent	$\delta^{18}O$	δD
40-55	61-80	7.11	4.47	0.59	5.64	-3.82	15.99
40-55	41-60	6.11	3.79	0.61	5.53	-4.27	70.34
40-55	41-60	11.82	7.41	0.60	5.20	-4.81	50.67
40-55	0-20	8.27	5.14	0.61	5.39	-3.97	1.88
40-55	61-80	10.91	6.83	0.60	5.72	-5.49	70.69
40-55	0-20	43.93	28.55	0.54	5.00	-3.89	11.59
40-55	0-20	20.52	12.91	0.59	5.80	-4.39	23.81
40-55	21-40	25.31	16.24	0.56	4.92	-4.62	41.79
40-55	41-60	32.69	20.53	0.59	5.51	-4.49	38.83
40-55	0-20	10.83	6.7	0.62	6.01	-4.94	55.69
40-55	21-40	15.28	9.65	0.58	6.22	-4.72	50.49
40-55	61-80	12.84	8.26	0.55	6.39	-4.75	57.87
40-55	0-20	19.02	11.96	0.59	6.54	-4.93	61.28
40-55	0-20	15.63	9.79	0.60	5.68	-4.30	25.85
40-55	0-20	16.05	10.12	0.59	6.04	-4.38	35.49
40-55	0-20	10.16	6.4	0.59	5.25	-4.48	42.12
40-55	21-40	24.41	15.3	0.60	5.96	-4.44	31.65
40-55	41-60	18.5	11.71	0.58	5.94	-4.51	55.30
40-55	0-20	20.28	12.73	0.59	6.46	-4.06	10.30
40-55	21-40	8.36	5.27	0.59	5.16	-4.03	16.80
40-55	61-80	18.75	12.08	0.55	5.62	-3.85	10.35
40-55	0-20	30.52	19.35	0.58	6.26	-4.06	4.95
40-55	21-40	25.82	17.1	0.51	5.13	-3.73	16.18
40-55	0-20	28.71	18.47	0.55	6.11	-4.04	7.57
55-75	21-40	19.55	12.93	0.51	5.29	-4.51	12.75
55-75	81-100	22.79	14.66	0.55	5.26	-5.20	2.00
55-75	21-40	5.76	3.51	0.64	5.52	-3.07	23.51

(table B.5. cont'd)

Depth (cm)	Percent Dye Coverage	Wet Weight	Oven Dry Weight	Gravimetric Water Content	Organic Matter Percent	$\delta^{18}O$	δD
55-75	61-80	28.7	17.97	0.60	5.51	-4.62	15.20
55-75	61-80	22.34	14.59	0.53	5.31	-5.18	6.88
55-75	41-60	36.61	23.27	0.57	5.19	-4.76	4.93
55-75	41-60	30.47	19.59	0.56	5.40	-4.73	8.44
55-75	21-40	13.74	8.74	0.57	5.39	-4.14	12.29
55-75	0-20	12.64	8.03	0.57	4.74	-4.11	-0.77
55-75	0-20	46.39	30.82	0.51	5.27	-4.34	13.53
55-75	81-100	13.84	8.61	0.61	5.24	-4.56	7.08
55-75	21-40	13.39	8.1	0.65	5.01	-4.65	1.25
55-75	81-100	5.6	3.57	0.57	4.84	-3.14	7.69
55-75	41-60	48.33	30.46	0.59	5.13	-4.69	2.51
55-75	81-100	12.14	7.81	0.55	4.81	-5.03	64.15
55-75	61-80	11.56	7.34	0.57	5.88	-4.13	12.27
55-75	0-20	30.67	19.53	0.57	4.84	-4.47	-2.26
55-75	0-20	11.63	7.46	0.56	5.01	-3.99	7.08
55-75	61-80	52.59	33.65	0.56	5.76	-4.43	6.38
55-75	21-40	23.4	14.71	0.59	5.34	-4.33	11.86
55-75	21-40	26.78	17.23	0.55	5.42	-4.06	4.95
55-75	21-40	24.3	15.3	0.59	5.32	-4.06	4.95
55-75	61-80	12.71	7.92	0.60	5.52	-3.64	6.39
55-75	0-20	17.68	11.08	0.60	5.53	-3.68	-1.26
55-75	21-40	24.16	15.49	0.56	5.47	-3.92	28.90
55-75	41-60	44.03	28.14	0.56	5.61	-3.53	6.14

Table B.6. Long treatment duration ped data including physical properties and isotopic values.

Depth (cm)	Percent Dye Coverage	Wet Weight	Oven Dry Weight	Gravimetric Water Content	Organic Matter Percent	$\delta^{18}O$	δD
0-4	41-60	6.74	4.09	0.65	7.85	-3.90	72.12
0-4	41-60	5.89	3.4	0.73	8.67	-4.23	73.94
0-4	81-100	2.96	1.54	0.92	13.50	-3.97	69.47
0-4	81-100	11.23	6.46	0.74	10.22	-3.75	78.73
0-4	81-100	8.52	5.07	0.68	8.07	-3.67	77.84
0-4	61-80	7.7	4.37	0.76	10.28	-3.67	75.90
0-4	81-100	4.99	2.95	0.69	8.11	-4.02	75.47
0-4	81-100	5.21	3.23	0.61	6.66	-3.71	74.95
0-4	81-100	11.24	6.33	0.78	10.13	-3.51	74.51
0-4	81-100	10.65	6.12	0.74	9.50	-3.32	78.45
0-4	61-80	19.66	12.17	0.62	7.97	-3.64	74.59
0-4	81-100	12.07	6.54	0.85	12.50	-4.18	78.23
0-4	81-100	3.53	2.16	0.63	7.28	-4.09	71.05
0-4	61-80	4.71	2.88	0.64	7.62	-4.22	72.01
0-4	61-80	5.57	3.18	0.75	10.72	-4.04	71.80
0-4	81-100	6.22	3.38	0.84	13.75	-3.93	77.06
0-4	61-80	9.72	6.03	0.61	6.65	-4.00	72.80
0-4	81-100	5.14	3.04	0.69	9.04	-3.80	74.44
0-4	61-80	23.02	13.49	0.71	9.94	-3.98	76.70
0-4	81-100	6.94	4.09	0.70	9.55	-4.20	77.18
0-4	81-100	12.19	7.29	0.67	9.80	-4.00	79.37
0-4	61-80	19.85	12.09	0.64	7.81	-4.17	77.44
0-4	81-100	4.7	2.84	0.65	9.46	-3.98	75.30
0-4	81-100	6.82	3.45	0.98	15.89	-4.33	74.90
0-4	81-100	7.43	4.4	0.69	8.94	-3.92	74.56

(table B.6. cont'd)

Depth (cm)	Percent Dye Coverage	Wet Weight	Oven Dry Weight	Gravimetric Water Content	Organic Matter Percent	$\delta^{18}O$	δD
0-4	61-80	5.94	3.62	0.64	7.29	-4.12	71.04
4-10	81-100	14.99	8.56	0.75	10.03	-4.12	76.95
4-10	41-60	16.56	9.97	0.66	7.89	-3.97	77.10
4-10	61-80	17.1	10.17	0.68	8.81	-3.74	75.53
4-10	0-20	7.34	4.55	0.61	7.17	-3.32	71.87
4-10	81-100	13.45	8.01	0.68	8.62	-3.80	77.89
4-10	61-80	33.84	20.5	0.65	8.80	-3.13	77.58
4-10	81-100	5.26	2.83	0.86	11.74	-3.94	72.38
4-10	21-40	22.79	13.89	0.64	7.61	-3.81	69.98
4-10	21-40	37.13	23.31	0.59	7.53	-3.68	66.00
4-10	21-40	43.48	26.94	0.61	8.13	-3.88	73.64
4-10	61-80	22.66	13.55	0.67	9.95	-4.02	77.07
4-10	61-80	44.44	27.58	0.61	8.56	-4.00	78.94
4-10	61-80	6.78	4.15	0.63	9.01	-4.18	68.60
4-10	61-80	17.83	10.69	0.67	9.63	-3.70	67.27
4-10	61-80	8.32	4.96	0.68	9.10	-4.20	73.73
4-10	41-60	18.81	11.56	0.63	7.49	-3.60	77.42
4-10	41-60	19.37	12.3	0.57	7.76	-4.20	76.79
4-10	41-60	7.23	4.33	0.67	10.43	-4.17	71.28
4-10	41-60	15.09	8.4	0.80	13.11	-4.17	77.47
4-10	41-60	14.24	8.92	0.60	8.49	-4.04	64.86
4-10	81-100	18.64	11.58	0.61	8.33	-4.28	76.86
4-10	41-60	27.41	16.73	0.64	7.78	-3.98	68.09
4-10	21-40	7.65	4.86	0.57	7.62	-4.23	66.66
4-10	61-80	27.31	16.32	0.67	8.81	-3.81	71.73
4-10	41-60	7.29	4.34	0.68	9.68	-3.64	70.45

(table B.6. cont’d)

Depth (cm)	Percent Dye Coverage	Wet Weight	Oven Dry Weight	Gravimetric Water Content	Organic Matter Percent	$\delta^{18}O$	δD
4-10	61-80	6.74	3.88	0.74	11.33	-3.84	72.60
4-10	81-100	9.33	5.51	0.69	8.75	-4.15	73.69
10-20	41-60	11.37	6.96	0.63	6.89	-3.74	66.61
10-20	81-100	5.74	3.34	0.72	7.91	-3.71	64.89
10-20	21-40	7.13	4.48	0.59	6.10	-3.40	54.77
10-20	21-40	8.21	5.07	0.62	7.72	-3.71	63.45
10-20	0-20	8.24	5.07	0.63	7.56	-3.67	70.51
10-20	61-80	21.61	13.7	0.58	7.32	-2.90	50.38
10-20	0-20	15.75	10.03	0.57	7.09	-3.43	57.12
10-20	81-100	20.66	12.88	0.60	6.65	-3.43	71.58
10-20	21-40	15.25	9.56	0.60	7.42	-3.30	60.01
10-20	61-80	16.19	10.01	0.62	7.62	-3.61	72.64
10-20	41-60	16.81	10.42	0.61	8.06	-3.15	54.26
10-20	61-80	21.77	13.92	0.56	7.77	-3.94	67.93
10-20	61-80	10.59	6.71	0.58	7.46	-3.83	55.06
10-20	81-100	11.21	7.07	0.59	8.61	-3.70	53.62
10-20	0-20	19.87	13.1	0.52	7.21	-3.56	45.27
10-20	21-40	12.77	8.22	0.55	6.37	-3.33	57.42
10-20	61-80	32.7	20.52	0.59	7.07	-3.90	65.90
10-20	61-80	12.34	7.67	0.61	7.55	-3.37	53.25
10-20	61-80	15.27	9.67	0.58	7.04	-3.77	60.60
10-20	41-60	27.07	17.54	0.54	6.88	-3.35	59.92
10-20	0-20	12.52	8.04	0.56	6.81	-3.70	63.65
10-20	41-60	7.81	4.88	0.60	8.07	-3.24	56.12
10-20	61-80	16.09	10.22	0.57	8.16	-4.14	70.02
10-20	21-40	17.43	11.16	0.56	8.43	-3.96	68.17
10-20	21-40	74.76	48.17	0.55	7.95	-3.46	54.42

(table B.6. cont'd)

Depth (cm)	Percent Dye Coverage	Wet Weight	Oven Dry Weight	Gravimetric Water Content	Organic Matter Percent	$\delta^{18}O$	δD
10-20	21-40	8.28	5.42	0.53	7.42	-3.60	52.17
10-20	21-40	35.42	21.75	0.63	8.42	-3.74	59.73
10-20	21-40	12.15	7.87	0.54	8.13	-3.98	70.18
10-20	21-40	14.38	8.87	0.62	8.43	-4.22	66.34
10-20	21-40	6.34	4.08	0.55	6.65	-4.12	55.22
10-20	0-20	12.68	8.2	0.55	7.22	-3.14	48.70
20-35	0-20	8.34	5.35	0.56	6.62	-3.63	46.73
20-35	21-40	25.11	13.65	0.84	6.84	-3.35	41.28
20-35	21-40	12.82	8.21	0.56	6.70	-3.08	51.42
20-35	21-40	33.07	21.29	0.55	5.93	-2.75	42.32
20-35	0-20	25.31	16.37	0.55	6.60	-3.24	47.86
20-35	61-80	12.78	8.29	0.54	6.74	-3.44	44.71
20-35	21-40	43.03	28.02	0.54	7.44	-3.47	65.36
20-35	0-20	14.4	9	0.60	6.07	-3.75	43.07
20-35	21-40	7.36	4.74	0.55	6.22	-3.17	39.75
20-35	41-60	20.33	13.45	0.51	6.33	-3.74	37.99
20-35	0-20	19.94	13	0.53	7.45	-3.57	33.27
20-35	0-20	10.87	7.06	0.54	6.81	-3.80	45.87
20-35	41-60	17.12	11.58	0.48	6.22	-3.69	41.49
20-35	0-20	17.12	10.75	0.59	6.47	-4.00	52.71
20-35	61-80	10.1	6.31	0.60	6.48	-3.67	39.99
20-35	41-60	25.38	15.8	0.61	6.81	-3.89	51.25
20-35	21-40	24.34	15.55	0.57	7.68	-3.43	28.90
20-35	21-40	12.01	7.63	0.57	7.36	-3.26	48.25
20-35	21-40	10.82	7.03	0.54	7.61	-3.32	28.26
20-35	21-40	18.97	12.11	0.57	6.81	-3.42	41.38
20-35	0-20	32.1	20.36	0.58	6.88	-3.38	40.89

(table B.6. cont'd)

Depth (cm)	Percent Dye Coverage	Wet Weight	Oven Dry Weight	Gravimetric Water Content	Organic Matter Percent	$\delta^{18}O$	δD
20-35	41-60	27.25	17.76	0.53	6.88	-3.57	39.48
20-35	0-20	29.94	19.24	0.56	6.90	-3.86	40.53
20-35	41-60	24.32	16.05	0.52	7.35	-3.73	51.84
20-35	61-80	13.27	8.6	0.54	7.39	-4.10	54.81
20-35	0-20	24.87	16.22	0.53	6.96	-4.51	58.35
20-35	0-20	16.86	10.96	0.54	6.99	-3.59	38.02
20-35	0-20	22.38	14.25	0.57	6.61	-4.00	52.53
20-35	41-60	11.87	7.53	0.58	7.60	-3.38	40.10
20-35	21-40	13.15	8.47	0.55	7.52	-3.47	46.27
20-35	41-60	11.57	7.27	0.59	7.84	-2.85	28.85
20-35	0-20	8.53	5.52	0.55	7.51	-3.29	44.07
40-55	0-20	9.47	5.92	0.60	5.72	-4.09	67.27
40-55	0-20	10.79	6.81	0.58	5.86	-4.07	65.44
40-55	0-20	10.38	6.5	0.60	6.19	-3.85	65.47
40-55	21-40	19.78	12.29	0.61	6.56	-4.01	70.65
40-55	21-40	8.77	5.53	0.59	5.90	-4.00	64.50
40-55	61-80	5.33	3.28	0.62	5.59	-3.99	64.00
40-55	0-20	6.27	3.93	0.60	5.82	-4.23	67.87
40-55	0-20	4.52	2.77	0.63	6.04	-4.15	65.98
40-55	0-20	26.93	17.06	0.58	6.62	-4.29	68.99
40-55	21-40	15.15	9.5	0.59	6.24	-4.40	70.20
40-55	21-40	9.76	6.11	0.60	6.91	-4.51	71.96
40-55	21-40	11.05	7.07	0.56	6.20	-4.35	59.66
40-55	61-80	7.64	4.61	0.66	6.48	-4.61	64.58
40-55	0-20	5.44	3.49	0.56	6.49	-4.08	59.39
40-55	0-20	8.36	5.25	0.59	6.52	-4.66	65.33
40-55	21-40	20.3	12.86	0.58	6.70	-4.84	71.83

(table B.6. cont'd)

Depth (cm)	Percent Dye Coverage	Wet Weight	Oven Dry Weight	Gravimetric Water Content	Organic Matter Percent	$\delta^{18}O$	δD
40-55	21-40	9.29	5.78	0.61	6.11	-4.66	59.45
40-55	21-40	14.41	9.12	0.58	6.50	-5.01	63.36
40-55	21-40	6.3	3.86	0.63	6.22	-4.74	66.17
40-55	61-80	7.81	4.81	0.62	5.94	-5.09	69.20
40-55	0-20	5.14	3.22	0.60	6.14	-4.73	61.85
40-55	0-20	10.72	6.72	0.60	5.95	-5.16	67.26
40-55	0-20	19.76	12.03	0.64	6.28	-5.03	68.50
40-55	41-60	21.69	13.83	0.57	6.20	-5.11	69.64
40-55	0-20	18.45	11.47	0.61	6.57	-5.39	71.25
40-55	21-40	12.22	7.73	0.58	6.24	-4.79	60.57
40-55	21-40	9.93	6.41	0.55	6.13	-4.66	66.93
40-55	41-60	30.36	19.51	0.56	6.06	-4.91	58.80
40-55	0-20	21.82	13.86	0.57	6.31	-4.99	69.65
40-55	0-20	52.76	33.72	0.56	6.17	-4.51	63.51
55-75	21-40	12.71	7.74	0.64	5.63	-3.76	42.44
55-75	21-40	19.83	12.23	0.62	6.52	-4.01	47.94
55-75	0-20	11.12	6.81	0.63	5.59	-3.62	44.38
55-75	61-80	2.85	1.72	0.66	5.90	-3.68	46.26
55-75	21-40	17.64	11.01	0.60	6.42	-3.87	49.30
55-75	21-40	23.82	15.28	0.56	5.68	-3.83	40.57
55-75	21-40	10.24	6.37	0.61	6.77	-3.98	55.82
55-75	0-20	13.69	8.42	0.63	6.25	-4.18	40.37
55-75	21-40	24.58	15.32	0.60	6.23	-3.75	41.52
55-75	21-40	21.11	12.98	0.63	6.00	-4.39	35.19
55-75	61-80	6.1	3.85	0.58	6.60	-4.42	48.32
55-75	61-80	25.76	16.66	0.55	5.35	-4.59	48.31
55-75	0-20	20.15	12.63	0.60	6.80	-4.44	48.84

(table B.6. cont’d)

Depth (cm)	Percent Dye Coverage	Wet Weight	Oven Dry Weight	Gravimetric Water Content	Organic Matter Percent	$\delta^{18}O$	δD
55-75	0-20	18.67	12.04	0.55	6.66	-4.59	43.13
55-75	21-40	20.98	13.18	0.59	6.09	-4.67	45.26
55-75	61-80	15.34	9.57	0.60	6.20	-4.85	46.90
55-75	81-100	7.26	4.46	0.63	8.33	-4.87	55.36
55-75	0-20	14.24	9.22	0.54	6.22	-4.81	38.85
55-75	0-20	13.45	8.69	0.55	6.00	-4.79	39.54
55-75	0-20	17.55	10.86	0.62	6.46	-5.04	54.30
55-75	21-40	10.15	6.19	0.64	6.43	-4.72	47.73
55-75	21-40	13.9	8.8	0.58	6.41	-5.02	52.10
55-75	61-80	15.25	9.27	0.65	6.01	-4.78	39.59
55-75	61-80	8.28	5.26	0.57	5.86	-4.74	35.03
55-75	21-40	26.77	17.09	0.57	6.19	-4.49	36.23
55-75	21-40	12.78	8.27	0.55	6.04	-4.52	38.33
55-75	41-60	14.4	9.06	0.59	6.26	-4.49	47.13
55-75	61-80	8.54	5.25	0.63	6.20	-4.51	52.49
55-75	0-20	56.44	36.79	0.53	5.91	-4.50	35.30
55-75	21-40	13.28	8.39	0.58	6.10	-4.29	34.73
55-75	41-60	14.86	9.34	0.59	6.33	-4.37	46.55

VITA

Savannah R. Morales is a native of Bayou Sorrel, Louisiana, a small fishing community on the east side of the Atchafalaya River Basin. She received her bachelor's degree in Renewable Natural Resources concentrating in wetland science at Louisiana State University in 2017. After graduation she continued her education in the School of Renewable Natural Resources at Louisiana State University working towards her master's degree concentrating in watershed science. She worked under the guidance of Dr. Richard Keim in the Forest and Wetland Ecohydrology Lab. She hopes to begin her career working in the same Louisiana wetlands she was raised in.